STOCHASTIC RESPONSE OF SINGLE DEGREE OF FREEDOM HYSTERETIC OSCILLATORS

by

G. O. Maldonado, M. P. Singh,
F. Casciati and L. Faravelli

Technical Report of Research Supported by
The National Science Foundation Under
Grant Number CEE-8412830

Department of Engineering Science and Mechanics
Virginia Polytechnic Institute and State University
Blacksburg, VA 24061

April 1987

BIBLIOGRAPHIC DATA SHEET	1. Report No. VPI-E-87-5	2.	3. Recipient's Accession No. PB88 232624/AS
4. Title and Subtitle Stochastic Response of Single Degree-of-Freedom Hysteretic Oscillators			5. Report Date April 1987 6.
7. Author(s) G. Maldonado, M. P. Singh, F. Casciati and L. Faravelli			8. Performing Organization Rept. No.
9. Performing Organization Name and Address Department of Engineering Science & Mechanics Virginia Polytechnic Institute & State Univ. Blacksburg, VA 24061			10. Project/Task/Work Unit No. 11. Contract/Grant No. CEE-8412830
12. Sponsoring Organization Name and Address National Science Foundation Washington, D.C. 20550			13. Type of Report & Period Covered Technical 14.

15. Supplementary Notes

16. Abstracts

During strong ground shaking structures often become inelastic and respond hysteretically. Therefore, in this study some hysteretic models commonly used in seismic structural analysis are studied. In particular the characteristics of a popular endochronic model proposed by Bouc and Wen are examined in detail. In addition, analytical expressions have also been developed for most commonly used bilinear model as well as another model, herein called as the hyperbolic model. As stochastic response analysis with such models commonly use the stochastic linearization approach which is necessarily iterative, here the convergence characteristics of such methods, when applied to calculate the response of single degree of freedom oscillators, are studied in detail. Several oscillators with different parameters are considered in the study. The ground motion is modeled by a stationary random process with Kanai-Tajimi spectral density function. It is noted that some adjustments in the equivalent linear parameters are necessary to achieve convergence. Also the rate of convergence to the final results is slower for the oscillators with low yield levels. The numerical results obtained by the equivalent linear approach are also compared with the results obtained for an ensemble of ground motion time histories and the possible causes of the discrepancy between the two results are discussed.

17. Key Words and Document Analysis. 17a. Descriptors

Nonlinear Analysis, Earthquakes, Seismic Response, Yielding, Hysteretic Behavior, Inelastic Response, Ductility Ratio, Structural Dynamics, Dynamic Response, Vibration, Linearization, Stochastic Linearization

17b. Identifiers/Open-Ended Terms

17c. COSATI Field/Group

18. Availability Statement	19. Security Class (This Report)	21. No. of Pages
Unlimited	UNCLASSIFIED	93
	20. Security Class (This Page) UNCLASSIFIED	22. Price

Acknowledgements

This report is the thesis of Gustavo O. Maldonado which was submitted to Virginia Polytechnic Institute & State University in April 1987 in partial fulfillment of the requirements of the degree of Master of Science in Engineering Mechanics.

This work is supported by National Science Foundation through Grant No. CEE-8412830. This financial support is gratefully acknowledged. The opinions, findings and conclusions or recommendations expressed in this report are those of the writers and these do not necessarily reflect the views of the National Science Foundation.

STOCHASTIC RESPONSE OF SINGLE DEGREE OF FREEDOM HYSTERETIC OSCILLATORS

by

Gustavo Omar Maldonado

Mahendra P. Singh

Engineering Mechanics

(ABSTRACT)

During strong ground shaking structures often become inelastic and respond hysteretically. Therefore, in this study some hysteretic models commonly used in seismic structural analysis are studied. In particular the characteristics of a popular endochronic model proposed by Bouc and Wen are examined in detail. In addition, analytical expressions have also been developed for most commonly used bilinear model as well as another model, herein called as the hyperbolic model.

As stochastic response analysis with such models commonly use the stochastic linearization approach which is necessarily iterative, here the convergence characteristics of such methods, when applied to calculate the response of single degree of freedom oscillators, are studied in detail. Several oscillators with different parameters are considered in the study. The ground motion is modeled by a stationary random process with Kanai-Tajimi spectral density function. It is noted that some adjustments in the equivalent linear parameters are necessary to achieve convergence. Also the rate of convergence to the final results is slower for the oscillators with low yield levels.

The numerical results obtained by the equivalent linear approach are also compared with the results obtained for an ensemble of ground motion time histories and the possible causes of the discrepancy between the two results are discussed.

Table of Contents

CHAPTER I: INTRODUCTION

The behavior of engineering structures which are affected by dynamic loads can not always be described by simple linear-elastic models, Fig. 1. In many cases, the structures have nonlinear and inelastic stiffness characteristics. Often such stiffness characteristics also have, what we call, memory; that is, the response of the system at a given time not only depends on the input at that time but also on the input and response at an earlier time. If the applied load is cyclic, the structural response may also be cyclic with dissipation of energy through hysteresis cycles. Structures subjected to strong ground shaking exibit such inelastic characteristics, and it is necessary to consider these in the calculation of seismic response.

In earthquake structural engineering, the constitutive law of inelastic structures has often been approximated by the popular elasto-perfectly-plastic model, Fig. 2, or by the bilinear model, Fig. 3. Tests on some structural elements have, however, demonstrated the need of using more complex multilinear models, like the Takeda's model shown in Fig. 4 and used for reinforced concrete. Several such models are being utilized now in dynamic analysis of structures subjected to earthquake induced ground motions. In such analyses, usually a step-by-step time history analysis is performed. Computer codes like DRAIN-2D [1] and ANSR-1 [2] have been developed to carry out such analyses. It has, however, been found difficult to utilize these discrete multilinear models in the stochastic response analysis of structures.

In addition to these discrete multilinear models, continuous models have also been developed to characterize the hysteretic force deformation characteristic of structural elements and materials. The earliest example of such a model is, probably, the Ramberg-Osgood model [3]. This model has been utilized to characterize the hysteretic behavior of soils in several soil dynamics studies [4, 5] in earthquake engineering. The utilization of this model for metal and concrete structures is, however, uncommon. For such structures, the continous model proposed by Iwan [6] and an endochronic model proposed by Bouc [7] have recently been utilized. Bouc's model has been modified and improved further to include the time dependent degradation and pinching effects commonly observed in structures subjected to earthquake induced ground motions. Another model similar to Bouc's has also been developed by Ozdemir [8] which was utilized by Bhatti and Pister [9] in optimization studies in seismic design of structures.

Because of the analytical simplicity, Bouc's model has been of special interest lately. It has been extensively used by Wen [10], Baber and Wen [11], Casciati and Faravelli [12], Casciati [13] and many others in their studies of stochastic response of structures subjected to stochastic loads. In these studies, the nonlinear differential equations associated with the constitutive law are linearized through the concept of stochastic linearization [14]. The coefficients of the linearized equation are functions of the response statistics, which are not known a priori. Some initial estimates of these coefficients are obtained which are then used in the calculation of the response from the linearized equations. The calculated response is then used to modify or improve the earlier estimates of the coefficients. This process is repeated till a convergence in the calculated response and coefficient values is acheived. Such approaches are thus iterative in nature.

In this work, the utilization of the endochronic model proposed by Bouc in stochastic seismic response evaluation of a simple oscillator subjected to random earthquake inputs is further studied. In Chapter II, the characteristics of various parameters of Bouc's model are studied. The limitations and appropriateness of this model in earthquake structural engineering are examined. Two new endochronic laws are also proposed. One of them uses hyperbolic trigonometric functions to model a softening system and the other models bilinear hysteresis loops. In Chapter III the ana-

lytical details of the equivalent linearization process used for calculating the response of an oscillator with nonlinear hysteretic spring, and subjected to stationary filtered white noise excitation at the base are provided. In Chapter IV the convergence characteristics of the iterative procedure used in the calculation of response are examined in detail. The comparison of the results obtained by the stochastic linearization with those obtained by the time history analysis for an ensemble of accelerograms is also given. The summary and concluding remarks are given in Chapter V.

CHAPTER II: HYSTERETIC MODELS

2.1 INTRODUCTION

In this chapter we will discuss the characteristics of some commonly used hysteretic force models. In particular the model proposed by Bouc and subsequently modified by Wen, Baber, etc., is discussed in detail. Based on the study of this model, analytical forms of two other models --the hyperbolic and the bilinear-- are proposed.

2.2 EQUATION OF MOTION AND RESTORING FORCE

In general the equation of motion of a single-degree-of-freedom (SDF) system can be written as follows:

$$m\ddot{x} + Q'(x, \dot{x}, t) = -m\ddot{x}_g \qquad (2.01)$$

Where $Q'(x, \dot{x}, t)$ is the general nonlinear hysteretic force; x is the relative displacement of the oscillator with respect to its moving base; $\dot{x}$ and $\ddot{x}$ are the relative velocity and acceleration respectively; m is the mass of the oscillator and $\ddot{x}_g$ is the ground acceleration. In the present study we will consider that the damping dependent restoring force is linear. Then, the equation of motion reduces to:

$$m\ddot{x} + c\dot{x} + Q(x, \dot{x}, t) = -m\ddot{x}_g \qquad (2.02)$$

Now Q represents the undamped nonlinear hysteretic term, which is a function of the displacement and velocity; c is the damping constant.

In standard form, this equation can also be written as:

$$\ddot{x} + (2\zeta_o \omega_o)\dot{x} + \frac{1}{m} Q(x, \dot{x}, t) = -\ddot{x}_g \qquad (2.03)$$

where ω_o is the preyielding natural frequency and ζ_o is the viscous damping ratio of the system defined as $\zeta_o = \frac{c}{2m\omega_o}$.

If the material is linear and elastic, $Q(x, \dot{x}, t)$ reduces to $Q(x) = kx$, where k is the elastic constant of the spring supporting the mass, called the stiffness coefficient. To include the hysteretic behavior along with linear behavior, Wen [15] has proposed the following expression to model the restoring force

$$Q(x, \dot{x}, t) = k[\alpha x + (1 - \alpha)z] \qquad (2.04)$$

where z is an auxiliary variable which has hysteretic characteristics. Thus the second part in the above equation represents a nonlinear element in parallel with a linear element represented by the first part. The constant α is a weighting constant representing the relative participations of the

linear and nonlinear terms. We will discuss the meaning of this parameter for three different models considered in this study.

The tangent stiffness for the nonlinear restoring force is defined as:

$$k_t = \frac{dQ}{dx} = k\left[\ \alpha + (1 - \alpha)\frac{dz}{dx}\ \right] \tag{2.05}$$

The stiffness when $z = 0$ is called as the initial stiffness. If we choose the auxiliary variable z such that $\frac{dz}{dx} = 1$ at $z = 0$, we obtain the following for the initial stiffness:

$$k_t^i = k\,[\,\alpha + (1 - \alpha)\,] = k \tag{2.06}$$

We can also define the final stiffness for such a model at the asymptotic value of z, when $\frac{dz}{dx} = 0$, as:

$$k_t^f = k\,[\,\alpha + 0\,] = k\alpha \tag{2.07}$$

Thus, the parameter α can be seen to be the ratio of the final stiffness to the initial stiffness:

$$\alpha = \frac{k_t^f}{k_t^i} \tag{2.08}$$

In the following we now discuss the characteristics of Bouc-Wen, hyperbolic and bilinear models.

2.3 BOUC-WEN MODEL

To model the hysteretic behavior through z in Eq. 2.04, Wen [10] proposed an endochronic law as follows:

$$\dot{z} = A\,\dot{x} - \gamma\,|\dot{x}|\,z\,|z|^{n-1} - \beta\,\dot{x}\,|z|^{n} \tag{2.09}$$

This model is a generalization of the model proposed by Bouc [7] which has been extensively used and modified by Wen [10, 15], Baber and Wen [11], Casciati [12] and Casciati and Faravelli [13] in their work.

This model has four parameters A, γ, β and n. The effect of these parameter values on the shape of the hysteretic curve has been discussed earlier by Baber and Wen [11]. Here we will re-analyze this model comprehensively to understand better the influence of its various parameters on the characteristics of the model.

For this we devide Eq. 2.09 by $\dot{x}$, to obtain:

$$\frac{dz}{dx} = A - |z|^{n}\left[\beta + \frac{\dot{x}z}{|\dot{x}z|}\gamma\right] \tag{2.10}$$

We now define the ultimate value of z as the value at which $\frac{dz}{dx} = 0$. By setting $\frac{dz}{dx} = 0$ in Eq. 2.10 we obtain:

$$|z_u| = \left[\frac{A}{\beta + \frac{\dot{x}z_u}{|\dot{x}z_u|}\gamma}\right]^{\frac{1}{n}} \tag{2.11}$$

Since the positive value of z_u corresponds to the positive $\dot{x}$ and negative to the negative $\dot{x}$, the term $\frac{\dot{x}z_u}{|\dot{x}z_u|}$ is equal to 1. this defines z_u as:

$$|z_u| = \left[\frac{A}{\beta + \gamma}\right]^{\frac{1}{n}} \tag{2.12}$$

It is seen from Eq. 2.10 that the slope dz/dx is equal to A at $z = 0$. By properly adjusting the value of k to define initial stiffness, we can choose $A = 1$. This will also permit us to define α as the ratio of the final stiffness to the initial stiffness.

2.3.1 GAMMA PARAMETER

Various branches of a hysteretic loop, such as these shown in Fig. 5, can be devided into outward and inward paths. The paths starting at $z = 0$ and going towards $\pm z_u$ will be called as the outward paths. For such paths the product $\dot{x}z$ is always positive, and thus Eq. 2.10 for $\dot{x}z > 0$ can be written as:

$$\frac{dz}{dx} = A - (\beta + \gamma)\,|z|^n \tag{2.13}$$

Likewise, the paths starting from the extreme position of z toward $z = 0$ will be called as the inward paths. For such paths, the product $\dot{x}z$ is always negative, and thus Eq. 2.10 for $\dot{x}z < 0$ becomes:

$$\frac{dz}{dx} = A - (\beta - \gamma)\,|z|^n \tag{2.14}$$

It is noted that for $\gamma = 0$, Eq. 2.13 and 2.14 are the same. That is, the outward and inward paths coalesce into a single path. This implies that the relationship between z and x is not hysteretic, although for $n > 1$ it is still nonlinear.

Let us now consider a case with $\beta > 0$, and examine the effect of varying γ. If we choose $\gamma > 0$, then the slope in the x-z plane defined by Eq. 2.14 will always be greater than the slope defined by Eq. 2.13. Thus, the shape of the hysteresis loop will be like those in Fig. 6 or Fig. 7, with the loop being traced in a clockwise direction. On the other hand, if we choose $\gamma < 0$, then in the x-z plane, the slope defined by Eq. 2.14 will always be smaller than the slope defined by Eq. 2.13. The hysteresis loop in this case will be as shown in Fig. 8 or Fig. 9, with the loop now

being traced in a counterclockwise direction. The counterclockwise loop is, however, not physically possible as it implies a negative dissipation of the energy. This means that the parameter γ should be positive, at least when β is positive.

A similar observation can also be made for the negative β values. We observe that when $\gamma > 0$, the loops will again be traced like in Fig. 06 or in Fig. 07. Whereas if $\gamma < 0$, the loops will be traced like in Fig. 08 or Fig. 09. Thus we can conclude that the parameter γ should always be positive, independently of the value taken by β

2.3.2 BETA PARAMETER

We now observe that the softening and hardening characteristics can be created by proper choice of β and γ values.

2.3.2.1 Softening model

For a softening model, the slope of outward paths must decrease with $|z|$. For this it is necessary that:

$$(\beta + \gamma) > 0 \qquad \text{or} \qquad \beta > -\gamma \tag{2.15}$$

Thus for softening stiffness characteristics, the parameter β could possibly take a negative value since γ is always positive.

Now, to obtain a softening model with inward-path slopes decreasing as $z \rightarrow 0$, we need that:

$$(\beta - \gamma) < 0 \qquad \text{or} \qquad \beta < \gamma \tag{2.16a}$$

Thus, to satisfy the conditions expressed by Eq. 2.15 and Eq. 2.16a it is necessary that $-\gamma < \beta < \gamma$. In such a case, the hysteresis loop will be as presented in Fig. 10.a.

To decrease the area under the hysteresis loop, we can choose an inward path with increasing slope as $z \rightarrow 0$. This can be achieved by choosing:

$$(\beta - \gamma) > 0 \qquad \text{or} \qquad \beta > \gamma \tag{2.16b}$$

In this case, satisfaction of Eq. 2.16b, i.e., $0 < \gamma < \beta$, will give us a loop traced in Fig. 10.b.

We can obtain a linear inward path by simply choosing $\beta = \gamma$.

2.3.2.2 Hardening model

Similarly, for hardening stiffness characteristics, the slope of the outward path should increase with $|z|$. This can be ensured by choosing

$$\beta + \gamma < 0 \qquad \text{or} \qquad \beta < -\gamma \tag{2.17}$$

However, unlike softening models there is only one possible shape in this case (see Fig. 10.c).

We can now summarize the effect of β and γ on the shape of the hysteresis loop. We observe that: 1) γ must be grater than or equal to zero. A value of $\gamma = 0$ implies nonhysteretic behavior. 2) To obtain softening models β must be greater than $-\gamma$. Since $\gamma > 0$, β can take positive or negative values. 3) To obtain a softening model with inward paths concave inside the loop, the β value must be between $-\gamma$ and γ. 4) To obtain a softening model with inward paths concave outside the loop, the β value must greater than γ. 5) To obtain hardening models, β must be less than $-\gamma$.

2.3.3 EXPONENT PARAMETER

We will now study the effect of changing the exponent parameter in the endochronic law. It was mentioned by Wen [15] that as $n \to \infty$, the endochronic law approaches the commonly used elasto-plastic model for the softening case. To show this analytically, we examine the softening model. For a softening outward path $(\beta + \gamma) > 0$. The expression for such path is:

$$\frac{dz}{dx} = A - |z|^n (\beta + \gamma) \tag{2.18}$$

Substituting for $(\beta + \gamma)$ in terms of z_u from Eq. 2.12, we obtain:

$$\frac{dz}{dx} = A - A \left| \frac{z}{z_u} \right|^n \tag{2.19}$$

As noted before, the slope at $z = 0$ is A. Futhermore we note that when n approaches infinity, the ratio (z/z_u) approaches zero as $|z| < |z_u|$. From Eq. 2.19 we note that in such a case the slope at any point (x, z) becomes equal to A, and the relationship between z and x is a straight line.

Similarly, we can obtain the slope on the inward path, defined by Eq. 2.14 as:

$$\frac{dz}{dx} = A - \frac{\beta - \gamma}{\beta + \gamma} \left| \frac{z}{z_u} \right|^n \tag{2.20}$$

This slope also approaches a constant value of A as n becomes large.

Thus, for $n = \infty$, both the outward and inward path become straight lines, giving rise to an elasto-plastic endochronic model in the x-z plane. For a finite value of α in Eq. 2.4, the restoring force is then defined by a bilinear hysteresis loop.

2.3.4 PATH EQUATIONS IN THE X-Z PLANE

Eq. 2.10 defines a set of differential equations for various paths of the endochronic law. Depending upon the values of $\dot{x}$ and z, we will obtain different equations for different paths from Eq. 2.10. Integration of these equations will provide the equations for these paths. For example, if $\dot{x} > 0$ and $z > 0$, the differential equation for one of the two outward paths becomes:

$$\frac{dz}{dx} = A - (\beta + \gamma)\, z^n \tag{2.21}$$

Integration of this will provide

$$\int_0^z \frac{dz'}{A - (\beta + \gamma)\, z'^n} = (x - x_0) \tag{2.22}$$

Where x_0 is the x-value when $z = 0$ The integration on the left hand side of Eq. 2.22 is difficult to evaluate for higher values of n. However, we can for n = 1 obtain explicit expressions for z as a function of x for various paths. For this case, Eq. 2.10 for all paths can be written as:

$$\frac{dz}{dx} = A + \delta z \tag{2.23}$$

Where δ takes on different values for different paths as:

$$\delta = -(\beta + \gamma) \quad \text{for} \quad \dot{x} > 0\,, \quad z > 0 \tag{2.24a}$$

$$\delta = -(\beta - \gamma) \quad \text{for} \quad \dot{x} < 0\,, \quad z > 0 \tag{2.24b}$$

$$\delta = +(\beta + \gamma) \quad \text{for} \quad \dot{x} < 0\,, \quad z < 0 \tag{2.24c}$$

$$\delta = +(\beta - \gamma) \quad \text{for} \quad \dot{x} > 0\,, \quad z < 0 \tag{2.24d}$$

Integrating Eq. 2.23 and solving for z, we obtain:

$$z = \frac{A}{\delta}\left[e^{\delta(x - x_0)} - 1\right] \tag{2.25}$$

Where at $x = x_0$, $z = 0$. For the four paths defined by various values of δ in Eq. 2.24, the following expressions are obtained:

Outward path: $\dot{x} > 0$, $z > 0$

$$z = \frac{A}{(\beta + \gamma)}\left[1 - e^{-(\beta+\gamma)(x - x_0)}\right] \tag{2.26a}$$

Inward path: $\dot{x} < 0$, $z > 0$

$$z = \frac{A}{(\beta - \gamma)}\left[1 - e^{-(\beta-\gamma)(x - x_0)}\right] \tag{2.26b}$$

Outward path: $\dot{x} < 0$, $z < 0$

$$z = \frac{-A}{(\beta + \gamma)}\left[1 - e^{(\beta+\gamma)(x - x_0)}\right] \tag{2.26c}$$

Inward path: $\dot{x} > 0$, $z < 0$

$$z = \frac{-A}{(\beta - \gamma)}\left[1 - e^{(\beta-\gamma)(x - x_0)}\right] \tag{2.26d}$$

For various possible values of β and γ for the softening and hardening models, these paths are schematically shown in Figs. 11 and 12. The boundaries between the softening and hardening cases, which correspond to the values of $\beta + \gamma = 0$ and $\beta - \gamma = 0$ are also shown in these figures. The equation for all these boundaries can be simply written as:

$$z = A\,(x - x_0) \tag{2.27}$$

By a proper selection of β and γ values, as discussed earlier, a variety of hysteresis loops can be traced. For $-\gamma < \beta < \gamma$, ($|\beta| < \gamma$), Eqs. 2.26a-d, will form the hysteretic loop shown in Fig. 13. Similarly, if $\beta = \gamma$, the loop shown in Fig. 14 is obtained.

2.3.5 ALTERNATIVE FORM OF THE MODEL

For a comparison of different hysteretic models, it is sometimes convenient to use the same ultimate value of z. This value for the Bouc-Wen model is defined by Eq. 2.12. We will now rewrite Eq. 2.09 with z_u as one of the model parameters.

We solve Eq. 2.12 for β in terms of z_u and γ as:

$$\beta = \frac{A}{|z_u|^n} - \gamma \tag{2.28}$$

Introducing this in Eq. 2.09, we obtain:

$$\dot{z} = A\left[1 - \left|\frac{z}{z_u}\right|^n\right]\dot{x} + \gamma\left(\dot{x}|z|^n - z|z|^{n-1}|\dot{x}|\right) \tag{2.29}$$

For the special case of $\beta = \gamma$, where the inward paths are linear, this expresion simplifies to:

$$\dot{z} = \frac{A}{2\ |z_u|^n}\left[\left(2|z_u|^n - |z|^n\right)\dot{x} - z|z|^{n-1}|\dot{x}|\right] \tag{2.30}$$

2.4 HYPERBOLIC HYSTERETIC MODEL

Representation of Bouc-Wen model by Eqs. 2.26a-d for various branches of the loop suggests the possibility of developing the analytical expressions for other hysteretic models. For this we choose appropriate expressions for the outward and inward paths. For a smooth transition between these two paths it is necessary that the slopes of these paths be the same at $z = 0$. To demonstrate this, we choose the following expressions for the outward and inward paths:

Outward path:

$$z = a \ \tanh[b\,(x - x_0)] \tag{2.31}$$

Inward path:

$$z = a \ \sinh[b\,(x - x_0)] \tag{2.32}$$

It is seen that both these functions are zero at $x = x_0$. Also, the slopes of these two functions at $x = x_0$ or $z = 0$ are the same and equal to:

$$\frac{dz}{dx} = ab \quad \text{at} \quad z = 0 \tag{2.33}$$

The differential equations of the two paths in the x-z plane are given by

Outward paths: $(\dot{x} > 0,\ z > 0)$ and $(\dot{x} < 0,\ z < 0)$

$$\frac{dz}{dx} = \frac{ab}{\cosh^2[b\,(x - x_0)]} = \frac{ab}{\cosh^2[\tanh^{-1}(z/a)]} \tag{2.34}$$

Inward paths: $(\dot{x} < 0,\ z > 0)$ and $(\dot{x} > 0,\ z < 0)$

$$\frac{dz}{dx} = ab \ \cosh[b\,(x - x_0)] = ab \ \cosh[\sinh^{-1}(z/a)] \tag{2.35}$$

The corresponding endochronic model is obtained as:

$$\frac{dz}{dt} = \frac{dz}{dx}\frac{dx}{dt} \tag{2.36}$$

Which for the two paths can be written as:

Outward path: $(\dot{x}z) > 0$

$$\dot{z} = a\,b\,\dot{x} \ sech^2\left[\tanh^{-1}\left(\frac{z}{a}\right)\right] \tag{2.37}$$

Inward path: $(\dot{x}z) < 0$

$$\dot{z} = a\,b\,\dot{x} \ \cosh\left[\sinh^{-1}\left(\frac{z}{a}\right)\right] \tag{2.38}$$

These two expressions can be combined into a single expression as:

$$\dot{z} = ab\dot{x}\left[f_1 + \left[\frac{1}{2}\right]\left[1 - \frac{z\dot{x}}{|z\dot{x}|}\right](f_2 - f_1)\right] \tag{2.39}$$

where $f_1 = sech^2[\tanh^{-1}(z/a)]$ and $f_2 = \cosh[\sinh^{-1}(z/a)]$.

This model will trace a hysteretic loop as shown in Fig. 15. Eq. 2.39, however, can only produce a softening system.

It is also possible to have linear inward path in this case by simply adopting the following equation in place of Eq. 2.38:

$$\dot{z} = a\,b\,\dot{x}, \quad (\dot{x}z) < 0 \tag{2.40}$$

Combination of Eq. 2.37 and 2.40 into a single equation gives:

$$\dot{z} = ab\dot{x}\left[f_1 + \left[\frac{1}{2}\right]\left[1 - \frac{z\dot{x}}{|z\dot{x}|}\right](1 - f_1)\right] \tag{2.41}$$

2.5 BILINEAR HYSTERETIC MODEL

Since the bilinear models have been very frequently used to define the restoring force, it is of interest here also to develop an analytical expression for such models. It is also necessary to have an elasto-plastic law for z in Eq. 2.04 to obtain a post-yielding slope of α. We will, therefore, discuss the formulation of an elasto-plastic model now.

Fig. 16 shows the elasto-plastic behavior of z versus x . It is noted that on the outward path A-B-C the time derivative of z can be simply written as:

$$\dot{z} = \frac{1}{2}\dot{x}\left[\frac{z_u - z}{|z_u - z|} + 1\right]; \quad \dot{x} > 0\,, \quad z > 0 \tag{2.42}$$

Where z_u is the maximum value. Similarly on the other outward path, D-E-F,

$$\dot{z} = \frac{1}{2}\dot{x}\left[\frac{z_u + z}{|z_u + z|} + 1\right]; \quad \dot{x} < 0\,, \quad z < 0 \tag{2.43}$$

Whereas on the inward paths F-A and C-D The time derivative of z is:

$$\dot{z} = \dot{x}\,; \quad z > 0\,, \quad \dot{x} < 0 \quad \text{and} \quad z < 0\,, \quad \dot{x} > 0 \tag{2.44}$$

All these equations can be combined into a single expression as follows:

$$\dot{z} = f_3 - [\dot{x} - f_3]\frac{1}{2}\left[\frac{z\dot{x}}{|z\dot{x}|} - 1\right] \tag{2.45a}$$

Where f_3 is defined by:

$$f_3 = \frac{|\dot{x}|}{2}\left[\frac{\left(\frac{z}{|z|}\right)z_u - z}{\left|\left(\frac{z}{|z|}\right)z_u - z\right|} + \frac{\dot{x}}{|\dot{x}|}\right] \tag{2.45b}$$

2.6 OSCILLATOR RESPONSE AND HYSTERETIC BEHAVIOR

In this section, we obtain the response of an oscillator subjected to some base motion time history. The three restoring force models discussed in previous sections have been used. The $z(t)$ and $x(t)$ responses were obtained from the solution of the following equations:

$$\ddot{x} + 2\zeta_0\omega_0 + \omega_0^2[\alpha x + (1 - \alpha)z] = -\ddot{x}_g \tag{2.46a}$$

$$\dot{z} = \dot{z}(\dot{x}, z) \tag{2.46b}$$

To solve these differential equations we used a step by step integrating procedure encoded in the routine I1A2F of Abaci's library written for personal computers.

Fig. 17 shows the x-z response of the oscillator for the base motion time history shown in the inset. The Bouc-Wen model with $\beta = .5$, $\gamma = 1.5$, $A = 1.$, $n = 1.$ and $\alpha = .25$ has been used to

define the restoring force. The response after point A on the curve is the free vibration response, as the base motion ceases at this point.

Fig. 18 shows almost complete hysteresis loops obtained for the three restoring force models discussed in previous sections. For the Bouc-Wen model, Eq. 2.09, for the hyperbolic model, Eq. 2.41, and for the bilinear, Eq. 2.45 were used. For comparison purposes the ultimate values z_u were kept the same in the three models. The base motion time history for this case is shown in the inset.

These complete loops fail to point out a serious drawback of the Bouc-Wen and hyperbolic models. The experiments on metals have shown that a partial loading-unloading path should be like the one shown in Fig. 19 and 20. After a partial unloading, the reloading should form a small loop to reach the asymptotic yield level. However, this is not the case with the Bouc-Wen and the hyperbolic models. It can be clearly seen from Fig. 21, where the partial unloading paths A-B and reloading path B-C do not intersect. This softening behavior during a reloading followed by a partial unloading has not been observed in the experimental tests on metals. Probably there also exist more fundamental physical or thermodynamical reasons for the behavior shown in Fig. 20, but the author is not aware of this.

CHAPTER III: EQUIVALENT LINEARIZATION

3.1 INTRODUCTION

In Chapter II, we presented the equation of motion of a single degree of freedom oscillator with a nonlinear hysteretic constitutive law. That equation along with the endochronic law forms a system of two differential equations. These equations can be rewritten in the following form:

$$\ddot{x} + 2\zeta_0 \omega_0 \dot{x} + \omega_0^2 [\alpha x + (1 - \alpha) z] = -\ddot{x}_g \tag{3.01a}$$

$$\dot{z} + g(\dot{x}, z) = 0 \tag{3.01b}$$

Where the natural frequency ω_0 and the conventional damping ratio ζ_0 are, respectively, defined as:

$$\omega_0 = \sqrt{\frac{k}{m}} \quad ; \quad \zeta_0 = \frac{c}{2\omega_0 m} \tag{3.02}$$

and k is the initial stiffness parameter, discussed in Chapter II.

We also solved Eqs. 3.01a and 3.01b for various models of $\dot{z}$, for a prescribed base motion time history $\ddot{x}_g$, by a step-by-step nonlinear equation solver. Here in this chapter, however, we are interested in obtaining the response of this system for $\ddot{x}_g$ defined stochastically.

A general solution of these equations for an arbitrarily defined $\ddot{x}_g$ is almost impossible to obtain, even for the simplest of the endochronic models. Therefore, researchers have tried to obtain some approximate solutions. For stochastically defined inputs, the stochastic linearization is commonly used. In this chapter we will discuss the linearized solution of these equations for the Bouc-Wen and the bilinear hysteretic models.

3.2 EQUIVALENT LINEARIZATION TECHNIQUE

The linearization techniques have been widely used in practice since the first proposal by Krylov and Bogoliubov [16]. For hysteretic models, Wen and others have used this technique extensively in the analysis of single and multiple degree of freedom structures subjected to random earthquake loading. Here we will reiterate some important steps utilized in the linearization technique, not because they are new but because of completeness of the topic discussed in this work.

For the solution of Eqs. 3.01, the nonlinear equation 3.01b is replaced by a linear equation as follows:

$$\dot{z} + C\dot{x} + Kz = 0 \tag{3.03}$$

Where K and C are the linearization constants, yet to be determined. This linearization introduces some error, ε

$$\varepsilon = g(\dot{x}, z) - C\dot{x} - Kz \tag{3.04}$$

The error ε is a stochastic process. To obtain some estimates of K and C, it is customary to minimize the mean square value of this error. This minimization requires that

$$\frac{\partial E[\varepsilon^2]}{\partial C} = \frac{\partial E[\varepsilon^2]}{\partial K} = 0 \tag{3.05}$$

Where $E[\,.\,]$ is the expected value of $[\,.\,]$. Substitution of Eq. 3.04 into 3.05 and slight simplification give the following two simultaneous equation for the coefficients K and C

$$C\ E[\dot{x}^2] + K\ E[z\dot{x}] = E[\dot{x}\, g(\dot{x}, z)] \tag{3.06}$$

$$C\ E[\dot{x}z] + K\ E[z^2] = E[z\, g(\dot{x}, z)] \tag{3.07}$$

These two equations can be solved for the coefficients as:

$$\begin{bmatrix} C \\ K \end{bmatrix} = [C_{\dot{x}z}]^{-1} \begin{bmatrix} E\ [\dot{x}\, g(\dot{x}, z)] \\ E\ [z\, g(\dot{x}, z)] \end{bmatrix} \tag{3.08}$$

Where $[C_{\dot{x}z}]$ is the correlation function matrix for variables $\dot{x}$ and z. For known joint probability density function of $\dot{x}$ and z, the expected values on the right hand side of Eq. 3.08 can be calculated in principle.

However, under some very general conditions fulfilled by the density function of $\dot{x}$ and z and also the function $g(\dot{x}, z)$, it has been shown by Atalik and Utku [14] that Eq. 3.08 can also be simplified to:

$$\begin{bmatrix} C \\ K \end{bmatrix} = \begin{bmatrix} E\left[\dfrac{\partial g}{\partial \dot{x}}\right] \\ E\left[\dfrac{\partial g}{\partial z}\right] \end{bmatrix} \tag{3.09}$$

The conditions to be satisfied by the density function $f(\dot{x}, z)$ and the function $g(\dot{x}, z)$ are:

1) $f(\dot{x}, z)$ is Gaussian.

2) $|g(\dot{x}, z)| < A\ e^{(\dot{x}^a + z^b)}$, for an arbitary A and for a , b < 2.

3) $g(\dot{x}, z)$ is well behaved and differentiable.

For $g(\dot{x}, z)$ defined by the Bouc-Wen, Hyperbolic and Bilinear models, the conditions (2) and (3) are satisfied. Thus if we can also assume that the joint density function of $\dot{x}$ and z is Gaussian, Eq. 3.9 can be applied to simplify the computations.

3.3 BOUC-WEN MODEL

Wen [15] has also provided explicit expressions for calculating C and K for the Bouc-Wen model. However, as it has been very instructive for the writer to prove Eq. 3.9 and obtain the explicit expressions for C and K, the details of this proof and derivation for $n = 1$ are given in the Appendix for completeness of record. The mentioned expressions for $n = 1$ are:

$$C = \sqrt{\frac{2}{\pi}} \left[\frac{\gamma\ E[\dot{x}z]}{\sigma_{\dot{x}}} + \beta \sigma_z \right] - A \tag{3.10}$$

$$K = \sqrt{\frac{2}{\pi}} \left[\gamma \sigma_{\dot{x}} + \frac{\beta\ E[\dot{x}z]}{\sigma_z} \right] \tag{3.11}$$

In addition, for $n > 1$ Wen [15] obtained the following expressions:

$$C = \gamma \frac{2^{n/2}}{\pi} \left[\sum_{r=0}^{n-1} \binom{n}{r} \Gamma_1\ \Gamma_2 \left[1 - \rho_{\dot{x}z}^2\right]^{r/2}\ \rho_{\dot{x}z}^{n-r}\ \sigma_z^n + \beta \frac{2^{n/2}}{\sqrt{\pi}}\ \Gamma_3\ \sigma_z^n \right] - A \tag{3.12}$$

$$K = \gamma \frac{2^{n/2}}{\pi} \left[\sum_{r=0}^{n-1} \binom{n-1}{r} \Gamma_1 \Gamma_2 \left[1 - \rho_{\dot{x}z}^2\right]^{r/2}\ \rho_{\dot{x}z}^{n-r+1} + \beta\, n \frac{2^{n/2}}{\sqrt{\pi}}\ \Gamma_3\ \rho_{\dot{x}z}\ \sigma_{\dot{x}}\ \sigma_z^{n-1} \right] \tag{3.13}$$

where σ_x, $\sigma_{\dot{x}}$ and σ_z are the standard deviations of the x, $\dot{x}$ and z responses, respectively and $\rho_{\dot{x}z}$ is the correlation coefficient of $\dot{x}$ and z In both equations Γ_i are the following Gamma functions:

$$\Gamma_1 = \Gamma\left[\frac{r+1}{2}\right], \quad \Gamma_2 = \Gamma\left[\frac{n-r+1}{2}\right], \quad \Gamma_3 = \Gamma\left[\frac{n+1}{2}\right]$$

Futhermore r must be an even integer.

3.4 BILINEAR MODEL

We can also obtain the equivalent linear coefficients for a bilinear model using Eqs. 3.09. In this case, the analytical expression for $g(\dot{x}, z)$ is given by Eq. 2.45. It is noted that for this case also, the function $g(\dot{x}, z)$ satisfies the conditions (2) and (3) given by Atalik and Utku. Again if we make the assumption that the joint density function is Gaussian, we can obtain the coefficients by Eq. 3.09.

The function $g(\dot{x}, z)$ in Eq. 2.45 can also be defined over the domain of $\dot{x}$ and z as follows:

$$g(\dot{x}, z) = \begin{cases} -\dot{x} & \text{for } 0 \le z \le z_u \text{ and } \dot{x} \ge 0 \\ 0 & \text{for } z \ge z_u \text{ and } \dot{x} \ge 0 \\ -\dot{x} & \text{for } z \ge 0 \text{ and } \dot{x} \le 0 \\ -\dot{x} & \text{for } -z \le z \le 0 \text{ and } \dot{x} \le 0 \\ 0 & \text{for } z \le -z_u \text{ and } \dot{x} \le 0 \\ -\dot{x} & \text{for } z \le 0 \text{ and } \dot{x} \ge 0 \end{cases} \tag{3.14}$$

In this domain the function is at least piecewise differentiable. The derivative required in Eq. 3.09 can be defined as:

$$\frac{\partial g(\dot{x}, z)}{\partial \dot{x}} = \begin{cases} -1 & \text{for } 0 \le z \le z_u \text{ and } \dot{x} \ge 0 \\ 0 & \text{for } z \ge z_u \text{ and } \dot{x} \ge 0 \\ -1 & \text{for } z \ge 0 \text{ and } \dot{x} \le 0 \\ -1 & \text{for } -z_u \le z \le 0 \text{ and } \dot{x} \le 0 \\ 0 & \text{for } z \le -z_u \text{ and } \dot{x} \le 0 \\ -1 & \text{for } z \le 0 \text{ and } \dot{x} \ge 0 \end{cases} \tag{3.15}$$

Also, it is noted that the function is independent of z in these discrete domains. Thus, its derivative with respect to z is zero. Substitution of these in Eq. 3.09 gives:

$$C = -\int_{-\infty}^{z_u}\int_{0}^{\infty} f_{\dot{x}z}(\dot{x}, z)\, dz\, d\dot{x} - \int_{-z_u}^{\infty}\int_{-\infty}^{0} f_{\dot{x}z}(\dot{x}, z)\, dz\, d\dot{x} \tag{3.16}$$

$$K = 0 \tag{3.17}$$

The integrals in Eq. 3.16 can be evaluated at least numerically and thus C can be defined. On the other hand the coefficient K is defined but its value being zero poses some problems in stationary equivalent linear response analysis. This is discussed later.

3.5 EQUIVALENT LINEAR STATIONARY RESPONSE

With the substitution of the equivalent linear expression for $g(\dot{x}, z)$ in Eq. 3.01b we get a set of coupled linear differential equations as follows:

$$\ddot{x} + 2\zeta_0 \omega_0 \dot{x} + \omega_0^2 [\alpha x + (1 - \alpha) z] = -\ddot{x}_g \tag{3.18}$$

$$\dot{z} + C\dot{x} + Kz = 0 \tag{3.19}$$

These equations can be written as a system of first order differential equations for the state vector defined as:

$$\bar{y} = \begin{bmatrix} x \\ z \\ \dot{x} \end{bmatrix} \tag{3.20}$$

The differential equation is:

$$\frac{d}{dt}\begin{bmatrix} x \\ z \\ \dot{x} \end{bmatrix} = \begin{bmatrix} 0 & 0 & 1 \\ 0 & -K & -C \\ -\alpha\omega_0^2 & -(1-\alpha)\omega_0^2 & -2\zeta_0\omega_0 \end{bmatrix}\begin{bmatrix} x \\ z \\ \dot{x} \end{bmatrix} + \begin{bmatrix} 0 \\ 0 \\ -\ddot{x}_g \end{bmatrix} \tag{3.21}$$

Often $\ddot{x}_g$ is defined as the output of a filter subjected to a white noise or shot noise as the input. In such cases we introduce another equation for the filter defined as:

$$\ddot{x}'_g + 2\zeta_g\omega_g\dot{x}'_g + \omega_g^2 x'_g = -\ddot{f}(t) \tag{3.22}$$

Where ω_g and ζ_g are the frequency and damping ratio parameters of the filter, x'_g is the relative displacement response of the filter with respect to the base and $\ddot{f}(t)$ is the acceleration at the base of the filter. This acceleration is assumed to be a delta correlated process.

The absolute acceleration response of this filter is the input $\ddot{x}_g$ in Eq. 3.18, that is,

$$\ddot{x}_g = \ddot{x}'_g + \ddot{f}(t) = -2\zeta_g\omega_g\dot{x}'_g - \omega_g^2 x'_g \tag{3.23}$$

Eqs. 3.18, 3.19 and 3.22 can now be combined into a single system of first order differential equations as:

$$\frac{d}{dt}\begin{bmatrix} x \\ z \\ \dot{x} \\ \dot{x}'_g \\ x'_g \end{bmatrix} = \begin{bmatrix} 0 & 0 & 1 & 0 & 0 \\ 0 & -K & -C & 0 & 0 \\ -\omega_0^2\alpha & -\omega_0^2(1-\alpha) & -2\zeta_0\omega_0 & 2\zeta_g\omega_g & \omega_g^2 \\ 0 & 0 & 0 & -2\zeta_g\omega_g & -\omega_g^2 \\ 0 & 0 & 0 & 1 & 0 \end{bmatrix} \begin{bmatrix} x \\ z \\ \dot{x} \\ \dot{x}'_g \\ x'_g \end{bmatrix} + \begin{bmatrix} 0 \\ 0 \\ 0 \\ -\ddot{f}(t) \\ 0 \end{bmatrix} \quad (3.24)$$

This system of Eqs. 3.21 or 3.24 can be written in a more compact form as:

$$\frac{d\tilde{y}}{dt} = G\tilde{y} + \tilde{F} \quad (3.25)$$

For a zero mean excitation, the expected value of $\tilde{y}$ will be zero. As shown by Lin [17], the differential equation for the covariance matrix of $\tilde{y}$ can be obtained as:

$$\frac{dS}{dt} = GS + SG^T + B \quad (3.26)$$

Where S is the covariance matrix of $\tilde{y}$ and B is a matrix with all its elements being zero except the diagonal element corresponding to the nonzero row of the forcing function vector in Eq. 3.21 and Eq. 3.24. The nonzero element of this matrix is defined as $2\pi G_0$, for a white noise with spectral density ordinate of G_0.

If we are interested in the stationary response, then the left hand side of Eq. 3.26 is zero. Thus, the stationary covariance matrix can be obtained from the solution of the following Liapunov's matrix equation:

$$GS + SG^T + B = 0 \quad (3.27)$$

A computer scheme developed by Bartels and Steward [18] was used in this study to solve this Liapunov's equation.

It is, however, noted that the equivalent linear coefficients C and K in this scheme are themselves defined in terms of the response which is not known a priori. To start the solution therefore some appropriate values are assumed for C and K, which are then used to define matrix G in Eq. 3.27. Solution of this equation provides the response covariances which are in turn used in the calculation of new values of C and K from Eqs. 3.10 and 3.11 or from 3.12 and 3.13 for the Bouc-Wen model. This iterative process is repeated till a convergence is achieved. The convergence characteristics of this procedure for the Bouc-Wen model are presented in the following chapter.

Implementation of this equivalent linear procedure in the calculation of stationary response covariance for a bilinear hysteretic model, however, has not been possible. This is because the coefficient K for this case is zero, which renders matrix G singular for this case. Thus, the numerical approach used with Eq. 3.27 can not be utilized. The nonstationary solution can still be obtained in principle. This will be attempted in future investigations.

CHAPTER IV: NUMERICAL RESULTS

4.1 INTRODUCTION

As mentioned in the previous chapter, the stochastic linearization approach is necessarily iterative. In this chapter we will consider the convergence characteristics of the linearization approach. The linearization coefficients of the nonlinear equation depend upon the response, which in turn is not known a priori. The process, thus, starts with some assumed values of the linearization coefficients and then is obtained the response. The calculated response is then used to calculate the new values of the coefficients which are then used again to calculate a new response value. The process is repeated till a desired convergence in the response quantities of interest is achieved.

The above procedure seems simple. Yet, some convergence problems were noted when no adjustments to the iterative process were made. It was also observed that the convergence also depended upon the parameters of the problem. In some cases as high as 39 number of iterations are required to achieve the desired level of convergence. In this Chapter, therefore, the experience gained in achiveing convergence to the final results is discussed. Numerical results showing the convergence rate for various cases are presented. Finally, the comparison of the response values

obtained by the stochastic linearization approach with the values obtained by the time history ensemble analysis are also presented and discussed.

4.2 PROBLEM PARAMETERS

The parameters considered in this study are the oscillator parameters, the parameters of the hysteresis model and the input motion parameters.

4.2.1 OSCILLATOR PARAMETERS

The oscillator parameters are: the initial frequency ω_0, the damping ratio ζ_0 and the yield level F_y. The oscillator frequencies ω_0 = 1, 1.5, 5, 6, 16 and 20 cps, and the damping ratios ζ_0 = 0.05 and 0.10 have been used. The yield displacement values of the stiffness element, y, were varied between .003 to .800 inches.

4.2.2 PARAMETERS OF THE HYSTERESIS MODEL

For the Bouc-Wen model, the parameters are β, γ and the exponent n. In all the cases $\beta = \gamma$ is assumed. The parameters β and γ are related to the yield level as follows. For the ultimate value of $z = z_u$, we obtained Eq. 2.28, which for $A = 1$ gives:

$$\beta + \gamma = \left(\frac{1}{z_u}\right)^n \tag{4.01}$$

For an equivalent bilinear model, the yield force at the yield displacement $x = y$ is given by

$$F_y = \alpha k y + k(1 - \alpha) z_y \tag{4.02}$$

Where z_y is the z-value at $x = y$. However, when $n \to \infty$, z_y approaches z_u, which in turn for $A = 1$ is equal to y. Thus in the limiting case of $n \to \infty$,

$$F_y = \alpha k y + k(1 - \alpha) y = k y = k z_u \tag{4.04}$$

Which gives

$$z_u = y = \frac{F_y}{k} \tag{4.05}$$

Substituting Eq. 4.05 into Eq. 4.01 we obtain:

$$\beta + \gamma = \frac{1}{y^n} \tag{4.06}$$

With the parameters β and γ choosen according to Eq. 4.06, in the limit, the restoring force defined as

$$Q = \alpha k x + k(1 - \alpha) z \tag{4.07}$$

will approach the bilinear case with initial stiffness of k, final stiffness of αk and yield displacement of y. With this equivalence in mind, the parameters β and γ are obtained from Eq. 4.06 for a given yield level.

As observed before in Chapter II, when n is increased, the hysteretic law approaches the bilinear case. Herein, the results are obtained for $n = 1$, 3 and 5. The convergence of the iterative process for the increasing values of n is extensively studied.

For an elastoplastic case, the post yielding stiffness parameter α should be equal to zero. However, this poses some problems in stochastic linearization as the matrix in Eq. 3.21 becomes singular and we cannot solve this equation in a stationary response case. The nonstationary re-

sponse can still be obtained, but it then depends upon the initial conditions. Analysis for such a case is more complicated and is not considered in this work. We have therefore, assumed as low values of α as possible without affecting the numerical accuracy of the results. For the elasto-plastic case, $\alpha = 1/21$, has often been assumed in stochastic linearization approaches in the past. We have used this value for obtaning the results for the elasto-plastic case, although some results with smaller values of α we also reported. For the bilinear hysteretic case, the numerical results with $\alpha = .25$ have been obtained.

4.2.3 INPUT MOTION PARAMETERS

The input to the oscillator is defined by a filtered white noise model. The most commonly used seismic input of this type is defined by the Kanai-Tajimi spectral density function of the following form:

$$\Phi_g(\omega) = S_0 \frac{\omega_g^4 + 4\zeta_g^2 \omega_g^2 \omega^2}{(\omega_g^2 - \omega^2)^2 + 4\zeta_g^2 \omega_g^2 \omega^2} \tag{4.08}$$

Where S_0 is the intensity of the white noise which establishes the level of exitation and ω_g and ζ_g are the ground filter parameters representing the frequency and damping ratio for the site. These two parameters were taken to be $\omega_g = 17.64$ rad/sec and $\zeta_g = .3535$

In the design of important structures, broad band inputs defined in terms of smoothed ground response spectra have often been used. The spectra presented by the U.S. Nuclear Regulatory Commission in Regulatory Guide 1.60 [19] for the design of Nuclear Power Plants are of this form. Spectral density functions which are consistent with such broad band spectra have also been used in practice. A model of spectrum consistent spectral density function proposed by Singh and Chu [20] is of the following form:

$$\Phi_g(\omega) = \sum_{i=1}^{3} S_i \frac{\omega_i^4 + 4\zeta_i^2 \omega_i^2 \omega^2}{(\omega_i^2 - \omega^2)^2 + 4\zeta_i^2 \omega_i^2 \omega^2} \tag{4.09}$$

This is the multimodal form of the Kanai-Tajimi spectral density function defined earlier. The parameters of this model used in this study are given in Table 1. This spectral density function gives the root mean square value (RMSV) of ground acceleration to be equal to 2.147 *ft/* sec^2. This with the peak factor value of 3.00 for ground acceleration random process, gives a peak ground acceleration of 6.44 *ft/* sec^2 or .2 *g*. The results obtained with this seismic input are compared with the results obtained by time history analysis for an ensemble of ground motion time histories scaled to .2*g* .

4.3 RATE OF CONVERGENCE RESULTS

The results for the rate of convergence obtained for several oscillators with different frequencies, damping ratios and yield level parameters are shown in Figs. 22 - 36. These curves are plotted for $n = 1, 3$ and 5. Each plot shows the logarithm (to the base 10) of the error versus the number of iterations. The error is defined as:

$$e = \left[\frac{|R_i - R_{i+1}|}{R_i} \right] \tag{4.10}$$

Where R_i and R_{i+1} are the mean square values of the response obtained at the i^{th} and $(i + 1)^{th}$ iteration. All three response quantities, x , $\dot{x}$ and z, were considered to obtain this error. Only the maximum error obtained among all three response quantities is shown in the plots. The convergence was assumed to have been achieved when this error was less than .01 for all response quantities.

Based in these results, it is felt that in a given problem the rate of convergence of the response to the final response primarily depended on the choice of the linearization parameters C and K. It has been suggested [22] that a value of $C = 1.0$ and $K = .05(\beta + \gamma)$ provides a better convergence. These initial values of C and K were observed to work very well with $n = 1$ and rather well with $n = 3$ in almost all cases. However for $n = 5$, some problems were observed. The experience showed that if the initial value of K was increased to be of order 1 (between 1 and 10), the convergence was assured in almost all cases.

Besides the choice of the initial values, it was also found to be important that the subsequent values of C and K, for following iterative steps, be chosen carefully. It was observed that if the C and K values, obtained according to Eqs. 3.10 and 3.11, were directly utilized then the convergence was not always assured. It was found desirable to choose C and K values somewhere in between the values obtained in the two consecutive steps. In fact, a simple average of the two values, if chosen as the value for the next step worked very well. That is, for the n^{th} step the initial values C_i and K_i calculated as:

$$C_i = \frac{C_{n-1} + C_n}{2} \tag{4.11}$$

$$K_i = \frac{K_{n-1} + K_n}{2} \tag{4.12}$$

expedited the convergence. Here C_{n-1} and K_{n-1} are the values used in the $(n-1)^{th}$ iterative step and C_n and K_n are the values calculated from Eqs. 3.10 and 3.11 in the n^{th} iterative step.

The convergence results were also obtained for two spectral density function models. It was observed that the type of input did not affect the convergence rate significantly. It was also observed that the rate of convergence was not affected by the choice of parameter α (see Fig. 37). As observed from Figs. 22 through 29, the rates of convergence are different for different yield level parameters. The number of iterations are seen to increase with a decrease in the yield level at which

the stiffness element will yield. That is, for the oscillators with large inelastic response or ductility ratio the number of iterations required for convergence will be large.

4.4 COMPARISON OF RESPONSE

In this section we compare the oscillator response results obtained by the equivalent linearization approach with those obtained for an ensemble of time histories.

The time history analysis results were obtained by Malushte [21]. For these results, the acceleration time histories representing the ground motion were synthetically generated for a spectral density function, the parameters of which are given in Table 1. These time histories were synthesized from randomly phased harmonics, with amplitudes determined from the spectral density function. The time histories were modified by a deterministic modulation function. These time histories had a total duration of 15 seconds with the strong motion phase of 4 seconds. In all a total of 75 such time histories were used. The maximum acceleration in each time history was normalized to a value of .2 g.

The numerical results were obtained for the elasto-plastic case with $\alpha = 0$ and for the bilinear case with $\alpha = .25$. Several yield levels were considered, as mentioned in the preceding section.

The time history response of each oscillator was obtained for each input motion time history. Thus, for each oscillator the ensemble containing 75 time histories was available to obtain the response statistics. From each response time history a maximum value was obtained which was then used to determine the mean maximum response. Here this mean of the maximum response value is compared with the mean of maxima obtained by the stochastic linearization technique. It is noted that individual maximum values for time histories did not occur at the same time.

In the stochastic linearization approach the mean of the maxima was obtained by multiplying the root mean square response value by the peak factor. The root mean square response value was obtained by a stationary random vibration analysis of the equivalent linear system.

The peak factor (PF) was calculated by the well-known Davenport formula [23] as:

$$PF = \sqrt{2 \ln\left(\frac{t_d \sigma_{\dot{x}}}{\pi \sigma_x}\right)} + \frac{.5772}{\sqrt{2 \ln\left(\frac{t_d \sigma_{\dot{x}}}{\pi \sigma_x}\right)}} \tag{4.13}$$

Where σ_x = standard deviation, $\sigma_{\dot{x}}$ = standard deviation of the response derivative and t_d is the equivalent stationary duration of the response. σ_x and $\sigma_{\dot{x}}$ are directly available from the random vibration analysis of the equivalent linear system. Since it is difficult to know the equivalent stationary duration for a nonstationary response, here two values of t_d = 4 sec. and t_d = 7 sec. were used to obtain the peak factors. The numerical results for the peak factor calculated with t_d = 4 sec. are given in Tables 2-5 and those for t_d = 7 sec. are given in Tables 6-9. The seismic input in the equivalent linear approach is defined by a white noise. To ensure that the input used in the time history approach is somewhat comparable with the input in the stochastic approach, a filter was added between the oscillator and the base. Thus, the input motion at the base of the oscillator was a filtered white noise of Kanai-Tajimi form. The numerical results for a single term Kanai-Tajimi spectral density function (Eq. 4.08, in which the filter with parameters in Table 1 is used) and the three-term Kanai-Tajimi spectral density function (Eq. 4.09, in which the three filters in parallel with parameters in Table 1 are used) are presented. The intensity of the white noise at the base of the filters was adjusted such that with a peak factor of 3, it gave a maximum ground acceleration of .2 g at the base of the oscillator.

As mentioned before, the nonlinear stiffness element in the stochastic approach is modeled by the Bouc-Wen model with exponent n = 1, 3 and 5. Since in a stationary response case we cannot obtain results for α = 0, for a elasto-plastic model, we have used α = 1/21 = .048 which has commonly been used in the literature. For the bilinear model, since the time history response

values are available for $\alpha = 1/4 = .25$, the stochastic results have also been obtained with this value.

Tables 2-9 show the results for various oscillators. Column 1 shows the oscillator identification number and columns 2, 3 and 4 show the oscillator parameters. The values in the remaining columns are for exponent $n = 1$, 3 and 5. For each case the following values are shown: the peak factor calculated by Davenport's formula, the maximum diplacement of the oscillator and the error between the maximum displacement value obtained by the equivalent linear approach and the time history ensemble results. This error is defined as:

$$Error = 100\frac{(x_t - x_s)}{x_t} \tag{4.14}$$

Where x_t and x_s are the mean of the maximum values obtained by time history and stochastic analysis approaches.

It is seen that the error is large in several cases and there is no particular trend, with respect to the choice of exponent, and the equivalent time duration t_d used in the calculation of the peak factors.

Probably a better comparison can be made by comparing the averages of the absolute errors in these tables. These averages are given in the last row. A comparison of these averaged errors shows that a smaller error is obtained for $\alpha = .25$ than for $\alpha = .048$. It is noted that the results for $\alpha = .25$ are for the same value of this parameter, both in the time history and stochastic approach. Whereas, the results for $\alpha = .048$ are for different values of this parameter in the time history and stochastic approach. In the time history the results are for $\alpha = 0$, and in the stochastic approach the results for $\alpha = .048$. It was not possible to obtain results for α values less than .048 because in the stochastic approach the numerical error in the results started to increase when α values less than .048 were used (see Fig. 38). Thus, it seems that a major share of the error in the results for

the elasto-plastic oscillators is due to our inability of modeling this case in the stationary stochastic approach.

Comparison of the average errors for one term and three term spectral density function inputs shows that the error in the latter case is smaller. This is probably due to the fact that the input of 3-term spectral density function is closer to the input used to define the acceleration time history in the time history analysis.

In conclusion it is felt that errors are large, though they can be improved by improving the proper modeling of the system and considering the nonstationarity of the response properly in the calculation of peak factors. To improve the accuracy of the stochastic linearization for the elasto-plastic case ($\alpha = 0$), it seems to be necessary to include the nonstationarity of the motion and response.

CHAPTER V: SUMMARY AND CONCLUSIONS

The motivation for this work was to study the characteristics of some nonlinear hysteretic models, commonly used in seismic structural analysis. In particular, here the model proposed by Bouc and Wen has been studied comprehensively. The effect of various model parameters on the characteristics of the model has been examined in detail in Chapter II. This study has led to the development of the analytical forms for two other hysteretic models, viz, hyperbolic model and bilinear model. It is expected that the expression for the bilinear model will be useful in future studies. The nonlinear response of oscillators with these three models has also been obtained for specified ground motion time histories. Some physical limitations of the commonly used Bouc-Wen model have also been identified.

In Chapter III, the equivalent linearization of the equation of motion of an oscillator with stiffness characterized by the Bouc-Wen model and by the bilinear model has been formulated. It is observed that it is not possible to work with the equivalent linear equations of the bilinear oscillator for calculating the stationary response. That is, to obtain any meaningful response in this case it is necessary to consider the initial conditions and the nonstationarity of the response. Such

a study is beyond the scope of this work. On the other hand, the Bouc-Wen model can still be used for stationary response calculations as long as the parameter α is nonzero.

In Chapter IV, numerical results have been obtained for oscillators with different characteristics to study the convergence behavior of the equivalent linear iterative approach. It is observed that the number of iterations required for convergence can indeed change with the parameters of the oscillators, such as frequency, yield level and the exponent parameter of the Bouc-Wen model. It is observed that the convergence is slowest for the exponent parameter value of $n = 5$. This convergence, however, can be improved by appropriately chosing the initial values of the linearization coefficients. It has been observed that better convergence is acheived when the initial values of the linearization coefficients for an iteration are taken as the average of the two recently calculated values. For oscillators with large inelastic response or ductility ratio the number of iterations required for convergence will be large. The rate of convergence does not seem to be affected by the other parameters of Bouc-Wen's model or the input characteristics.

The numerical results obtained by the equivalent linear approach are also compared with the results obtained for an ensemble of ground motion time histories. This comparison is not observed to be good; that is, for some oscillators the response values calculated by the equivalent linear approach differ significantly from the average values calculated by the time history ensemble analysies. The main reasons for this discrepancy are the inability of the equivalent linear approach (1) to precisely model the elasto-plastic and bilinear hysteretic models in the analysis, (2) to consider the nonstationarity of the input and response. The input in the equivalent linear approach is defined stochastically and assumed to be stationary. Whereas the time history inputs used in the time history calculations do not have stationary characteristics. In establishing the level of intensity of the stochastic input so that it gives the same maximum ground acceleration as the inputs in the time history analysis, some assumptions are made about the ground acceleration peak factors. These assumptions need to be verified. Also in calculating the peak response from the mean square response, the peak factors have been obtained from some simplified formulas which do not consider the nonstationarity of response. For a better corroboration of the two results it appears, therefore,

necessary that nonstationarity for the input and response be some how reflected in the calculation of response by the stochastic linearization approach.

APPENDIX

Derivation of Eq. 3.09

To prove Eq. 3.09, let us rename it as Eq. A.01:

$$\begin{bmatrix} C \\ K \end{bmatrix} = \begin{bmatrix} E\left[\frac{\partial g}{\partial \dot{x}}\right] \\ E\left[\frac{\partial g}{\partial z}\right] \end{bmatrix} \tag{A.01}$$

We first evaluate:

$$E\left[\frac{\partial g}{\partial \dot{x}}\right] = \int_z \int_{\dot{x}} \frac{\partial g}{\partial \dot{x}} f_{\dot{x}z}(\dot{x}, z)\ dx\ dz \tag{A.02}$$

Integration by parts of Eq. A.02 gives:

$$E\left[\frac{\partial g}{\partial \dot{x}}\right] = \int_z \left[g f_{\dot{x}z}(\dot{x}, z)\Big|_{-\infty}^{\infty} - \int_{\dot{x}} g \frac{\partial}{\partial \dot{x}} \left[f_{\dot{x}z}(\dot{x}, z)\right]\ d\dot{x} \right] dz \tag{A.03}$$

For the Bouc-Wen model and $n = 1$, the function $g(\dot{x}, z)$ is:

$$g(\dot{x}, z) = (\beta |z| - A)\dot{x} + \gamma |\dot{x}| z \qquad (A.04)$$

The first term on the right hand side of Eq. A.03 is obviously zero at the limits. Thus, Eq. A.03 becomes:

$$E\left[\frac{\partial g}{\partial \dot{x}}\right] = -\int_z \int_{\dot{x}} g \frac{\partial}{\partial \dot{x}}\left[f_{\dot{x}z}(\dot{x}, z)\right] d\dot{x}\ dz \qquad (A.05)$$

The joint distribution, if assumed Gaussian, can be written as:

$$f_{\dot{x}z}(\dot{x}, z) = \left[(2\pi)^2 \det\ [C_{\dot{x}z}]\right]^{-1/2}\ \exp\left[-\frac{1}{2}\tilde{U}^T\ [C_{\dot{x}z}]^{-1}\ \tilde{U}\right] \qquad (A.06)$$

Where $\tilde{U}^T = (\dot{x}, z)$. It is noted that because $|z|$ is limited to a maximum value of z_u, the assumption of the normality of the joint distribution is not correct. Nontheless, this assumption is commonly made. The derivative of Eq. A.06 can be written as:

$$\frac{\partial}{\partial \dot{x}}\left[f_{\dot{x}z}(\dot{x}, z)\right] = -\frac{1}{2} f_{\dot{x}z}(\dot{x}, z)\left[\frac{\partial \tilde{U}^T}{\partial \dot{x}}[C_{\dot{x}z}]^{-1}\tilde{U} + \tilde{U}^T[C_{\dot{x}z}]^{-1}\frac{\partial \tilde{U}}{\partial \dot{x}}\right] \qquad (A.07)$$

Since $\partial \tilde{U}^T/\partial \dot{x} = (1, 0)$, we can write:

$$\frac{\partial}{\partial \dot{x}}\left[f_{\dot{x}z}(\dot{x}, z)\right] = -f_{\dot{x}z}(\dot{x}, z)\begin{bmatrix}1\\0\end{bmatrix}^T [C_{\dot{x}z}]^{-1}\begin{bmatrix}\dot{x}\\z\end{bmatrix} \qquad (A.08)$$

Thus, from Eq. A.05:

$$E\left[\frac{\partial g}{\partial \dot{x}}\right] = \int_z \int_{\dot{x}} g f_{\dot{x}z}(\dot{x}, z)\begin{bmatrix}1\\0\end{bmatrix}^T [c_{\dot{x}z}]^{-1}\begin{bmatrix}\dot{x}\\z\end{bmatrix} d\dot{x}\ dz \qquad (A.09)$$

In a similar way we can obtain $E[\partial g/\partial z]$ as:

$$E\left[\frac{\partial g}{\partial z}\right] = \int_z \int_{\dot{x}} g f_{\dot{x}z}(\dot{x}, z) \begin{bmatrix} 0 \\ 1 \end{bmatrix}^T [C_{\dot{x}z}]^{-1} \begin{bmatrix} \dot{x} \\ z \end{bmatrix} d\dot{x}\ dz \qquad (A.10)$$

Combining Eq. A.09 and A.10, we obtain:

$$\begin{bmatrix} E\left[\frac{\partial g}{\partial \dot{x}}\right] \\ E\left[\frac{\partial g}{\partial z}\right] \end{bmatrix} = [C_{\dot{x}z}]^{-1} \int_z \int_{\dot{x}} g f_{\dot{x}z}(\dot{x}, z) \begin{bmatrix} \dot{x} \\ z \end{bmatrix} d\dot{x}\ dz \qquad (A.11)$$

Which means:

$$\begin{bmatrix} E\left[\frac{\partial g}{\partial \dot{x}}\right] \\ E\left[\frac{\partial g}{\partial z}\right] \end{bmatrix} = [C_{\dot{x}z}]^{-1} \begin{bmatrix} E[g\,\dot{x}] \\ E[g\,z] \end{bmatrix} \qquad (A.12)$$

Substituting for the vector on the right hand side of Eq. 3.08 from Eq. A.12, we obtain Eq. 3.09.

Expressions of C and K for Bouc-Wen's model with n = 1

To obtain the explicit expresions of C and K, we will use Eq. A.01. For the particular case of Bouc's model with exponent $n = 1$, the expression for $g(\dot{x}, z)$ is given in Eq. A.04. The derivatives of $g(\dot{x}, z)$ are:

$$\frac{\partial g}{\partial \dot{x}} = \gamma z \frac{\partial |\dot{x}|}{\partial \dot{x}} + \beta |z| - A \qquad (A.13)$$

$$\frac{\partial g}{\partial z} = \gamma |\dot{x}| + \beta \dot{x} \frac{\partial |z|}{\partial z} \qquad (A.14)$$

Considering Eq. A.01, A.13 and A.14, we can write the linearization coefficients as follows:

$$C = \gamma E\left[z\frac{\partial|\dot{x}|}{\partial\dot{x}}\right] + \beta E[|z|] - A \tag{A.15}$$

$$K = \gamma E[|\dot{x}|] + \beta E\left[\dot{x}\frac{\partial|z|}{\partial z}\right] \tag{A.16}$$

For the jointly Gaussian density function of $\dot{x}$ and z, it is straightfoward to obtain the expected values in Eq. A.15 and Eq. A.16 as:

$$E[|\dot{x}|] = \int_{\dot{x}} |\dot{x}|\, f_{\dot{x}}(\dot{x})\, d\dot{x} \tag{A.17}$$

Where

$$f_{\dot{x}}(\dot{x}) = \frac{1}{\sqrt{2\pi}\,\sigma_{\dot{x}}} \exp\left[\frac{-1}{2}\left[\frac{\dot{x}}{\sigma_{\dot{x}}}\right]^2\right] \tag{A.18}$$

Integrating, from $-\infty$ to ∞, we get:

$$E[|\dot{x}|] = \sqrt{\frac{2}{\pi}}\,\sigma_{\dot{x}} \tag{A.19}$$

In a similar way we can obtain $E[|z|]$:

$$E[|z|] = \sqrt{\frac{2}{\pi}}\,\sigma_z \tag{A.20}$$

To determine $E[z\ (\partial|\dot{x}|/\partial\dot{x})]$, we have to perform the following integrations:

$$E\left[z\frac{\partial|\dot{x}|}{\partial\dot{x}}\right] = \int_{\dot{x}} \frac{\partial|\dot{x}|}{\partial\dot{x}} \int_z z f_{\dot{x}z}(\dot{x}, z)\, dz\, d\dot{x} \tag{A.21}$$

Where

$$f_{\dot{x}z} = \frac{1}{2\pi\sigma_{\dot{x}}\sigma_z\sqrt{1-\rho^2}} \exp\left[-\frac{1}{2}\frac{1}{(1-\rho^2)}\left[\frac{\dot{x}^2}{\sigma_{\dot{x}}^2} - \frac{2\rho\dot{x}z}{\sigma_{\dot{x}}\sigma_z} + \frac{z^2}{\sigma_z^2}\right]\right] \qquad (A.22)$$

After integrating from $-\infty$ to ∞ the variable z, we get:

$$E\left[z\frac{\partial|\dot{x}|}{\partial\dot{x}}\right] = \frac{\rho\sigma_z}{\sigma_{\dot{x}}}\int_{-\infty}^{\infty}\frac{|\dot{x}|}{\sqrt{2\pi}\,\sigma_{\dot{x}}}\exp\left[-\frac{1}{2}\left[\frac{\dot{x}}{\sigma_{\dot{x}}}\right]^2\right]d\dot{x} \qquad (A.23)$$

Since the integrand in Eq. A.23 is the same as that in A.17, we can write:

$$E\left[z\frac{\partial|\dot{x}|}{\partial\dot{x}}\right] = \rho\sigma_z\sqrt{\frac{2}{\pi}} \qquad (A.24)$$

Where $\rho = \frac{E[\dot{x}z]}{\sigma_{\dot{x}}\sigma_z}$. Then,

$$E\left[z\frac{\partial|\dot{x}|}{\partial\dot{x}}\right] = \sqrt{\frac{2}{\pi}}\frac{E[\dot{x}z]}{\sigma_{\dot{x}}} \qquad (A.25)$$

Following a similar procedure, we find:

$$E\left[\dot{x}\frac{\partial|z|}{\partial z}\right] = \sqrt{\frac{2}{\pi}}\frac{E[\dot{x}z]}{\sigma_z} \qquad (A.26)$$

Substituting Eqs. A.19, A.20, A.25 and A.26 into A.15 and A.16, we obtain:

$$C = \sqrt{\frac{2}{\pi}}\left[\gamma\frac{E[\dot{x}z]}{\sigma_{\dot{x}}} + \beta\sigma_z\right] - A \qquad (A.27)$$

$$K = \sqrt{\frac{2}{\pi}}\left[\gamma\sigma_{\dot{x}} + \beta\frac{E[\dot{x}z]}{\sigma_z}\right] \qquad (A.28)$$

FIGURES

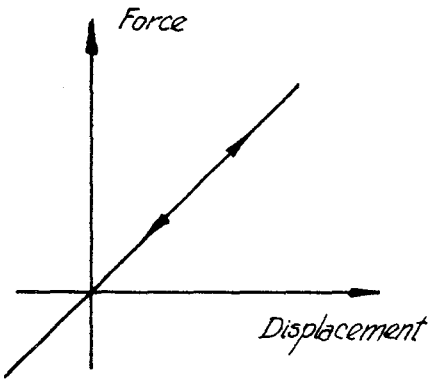

Fig. 1 LINEAR-ELASTIC MODEL

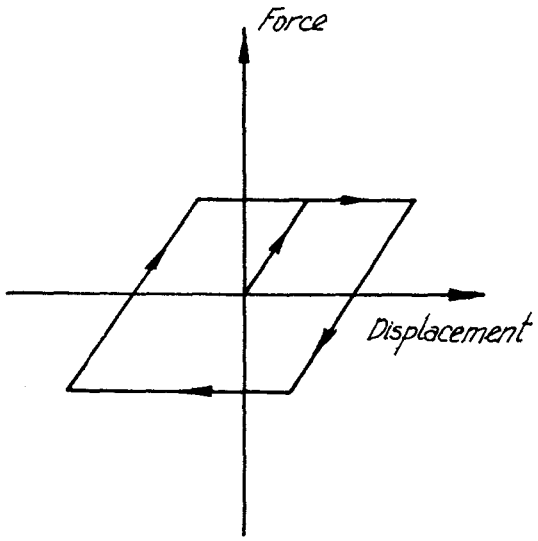

Fig. 2 ELASTO-PLASTIC MODEL

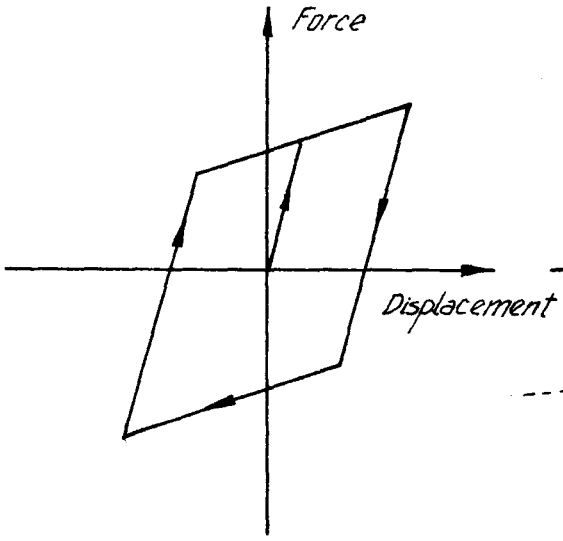

Fig. 3 BILINEAR MODEL

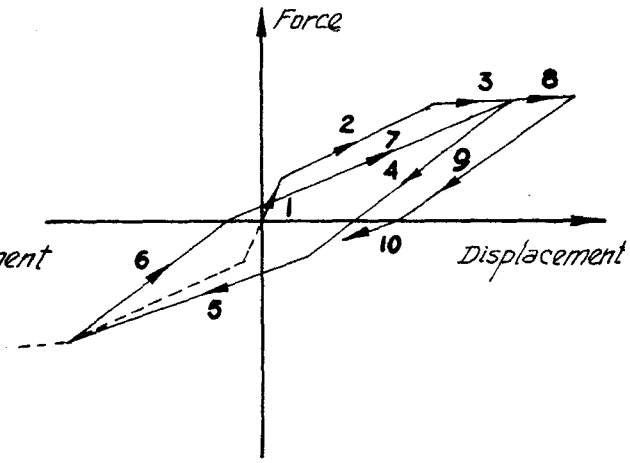

Fig. 4 TAKEDA'S MODEL

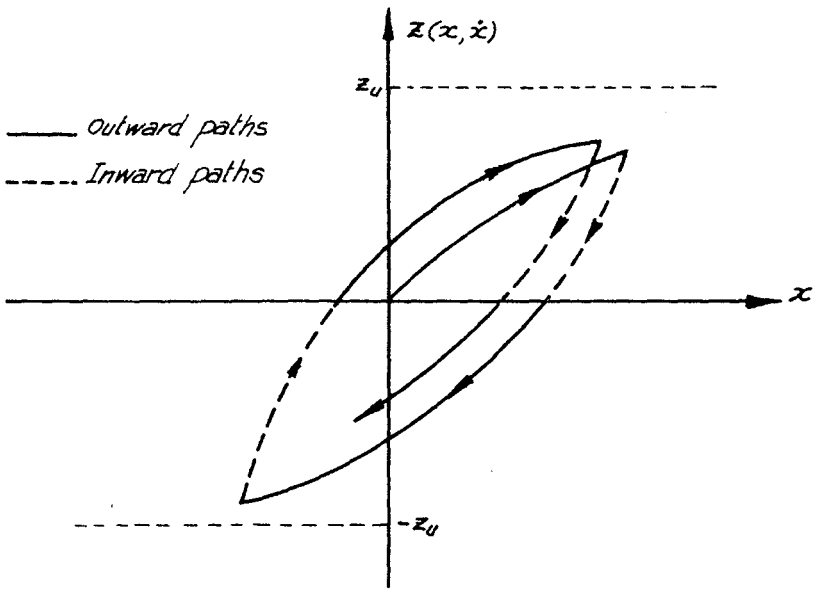

Fig. 5 OUTWARD and INWARD PATHS

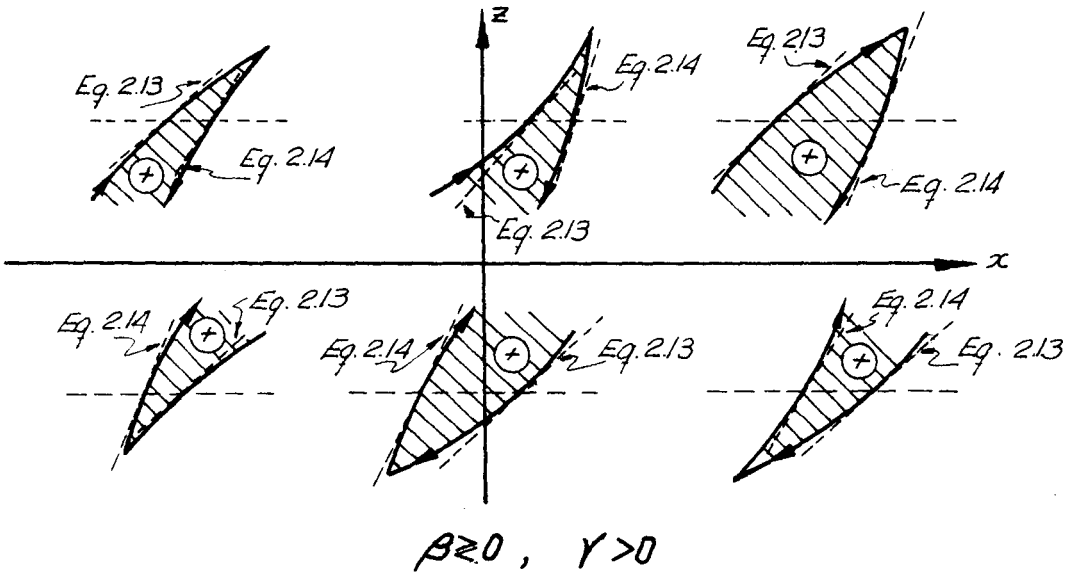

Fig. 6 SHAPE OF THE HYSTERESIS LOOPS

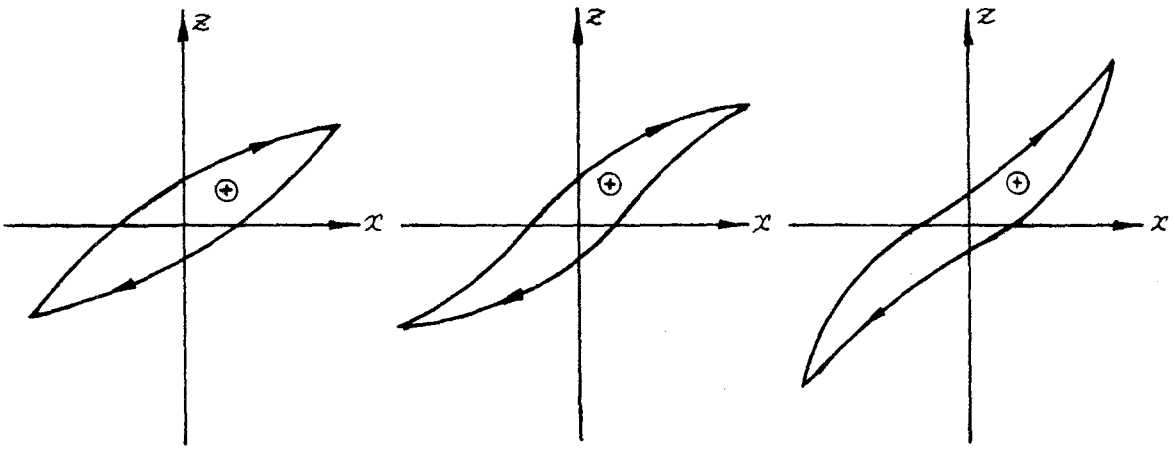

Fig. 7 LOOPS FOR $\gamma > 0$

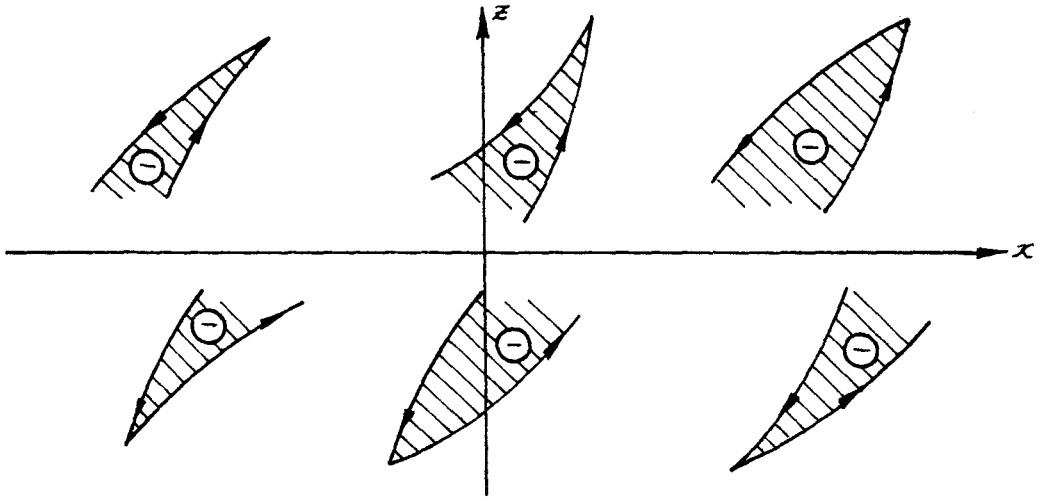

Fig. 8 SHAPE OF THE HYSTERESIS LOOPS

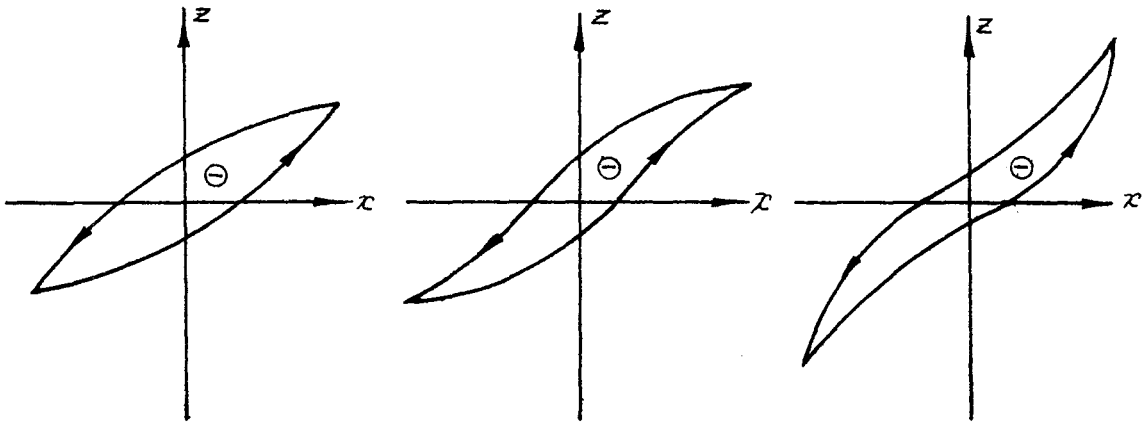

Fig. 9 LOOPS FOR $Y<0$

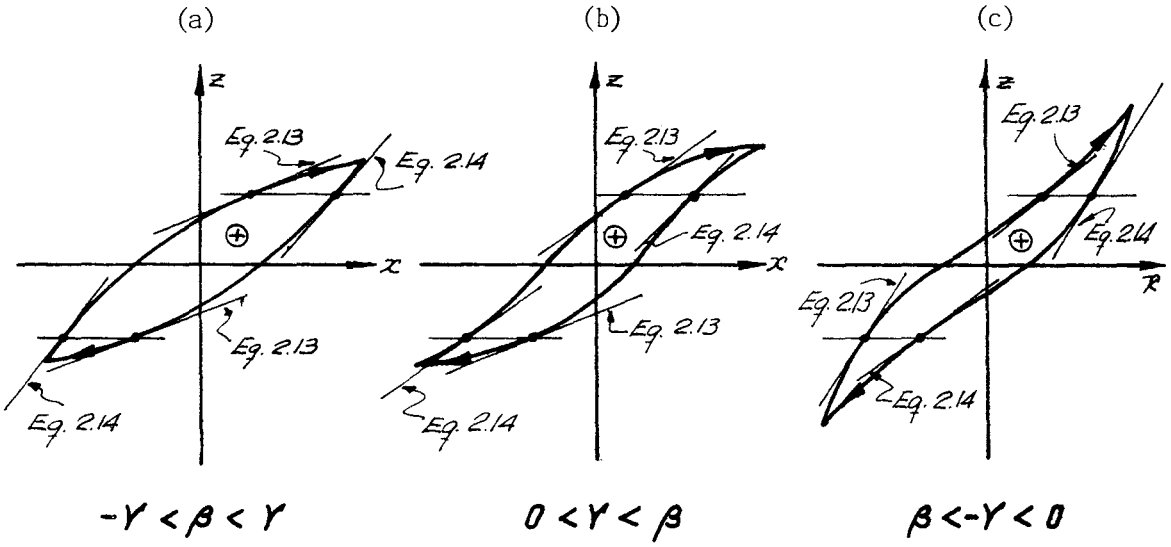

Fig. 10 SOFTENING and HARDENING MODELS

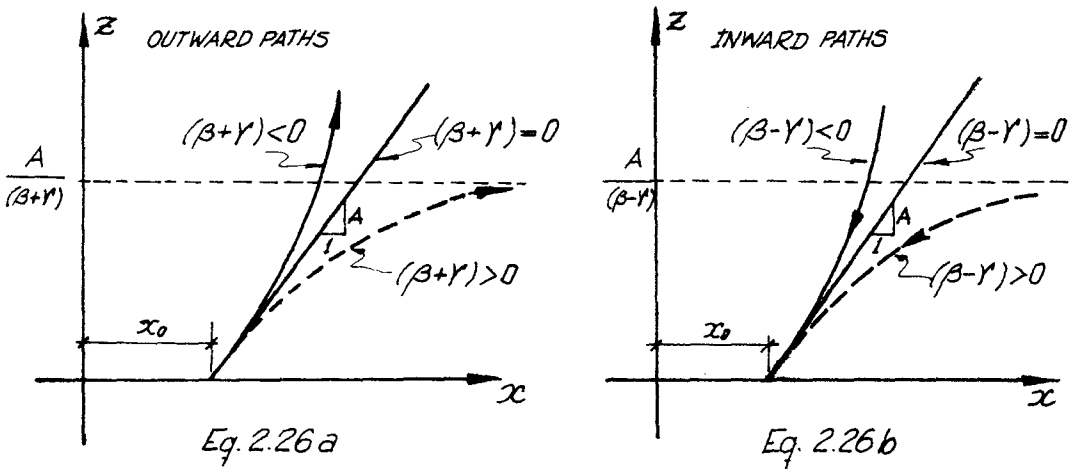

Fig. 11 PATHS FOR BOUC-WEN MODEL WITH n=1 and z>0

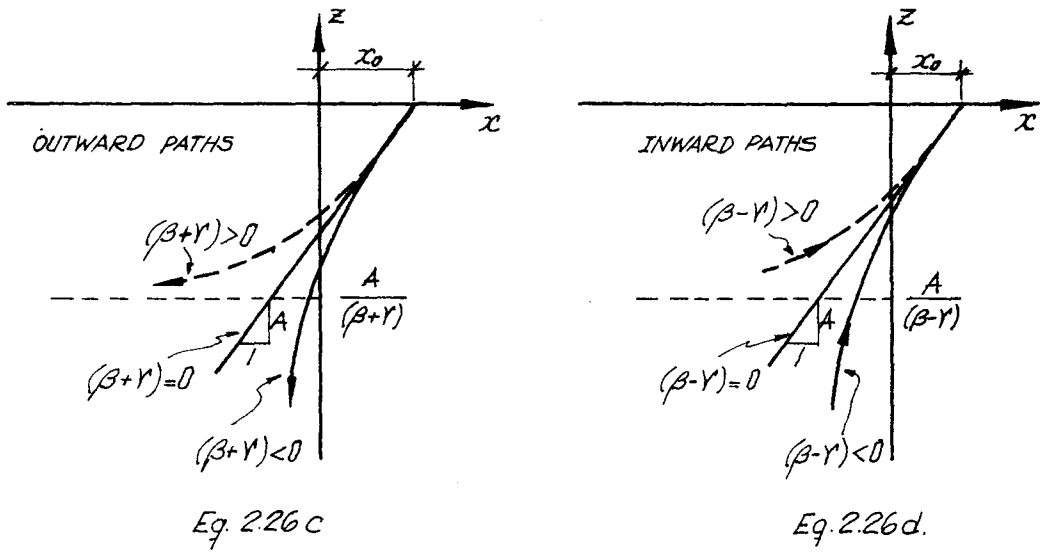

Fig. 12 PATHS FOR BOUC-WEN MODEL WITH n=1 and z<0

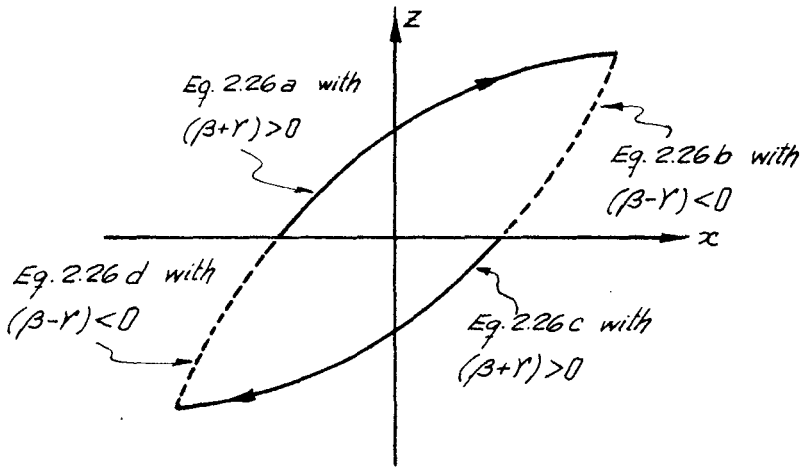

Fig. 13 BOUC-WEN MODEL with n = 1
and $-\gamma < \beta < \gamma$

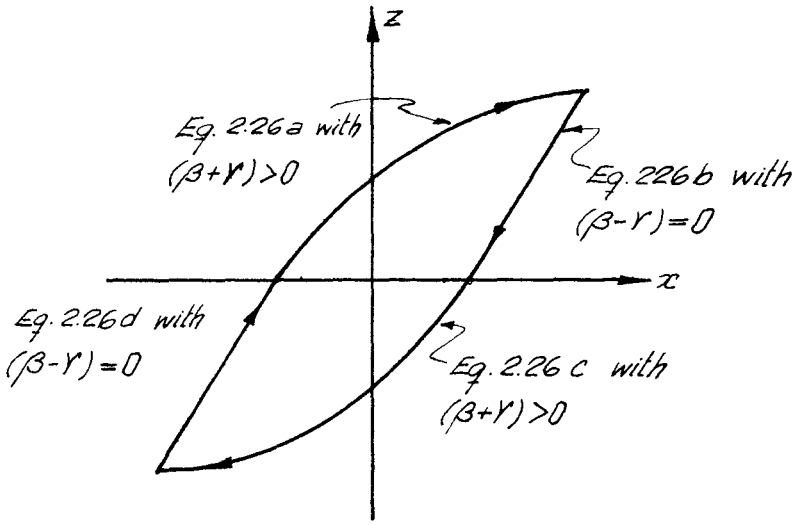

Fig. 14 BOUC-WEN MODEL with n = 1
and $0 < \beta = \gamma$

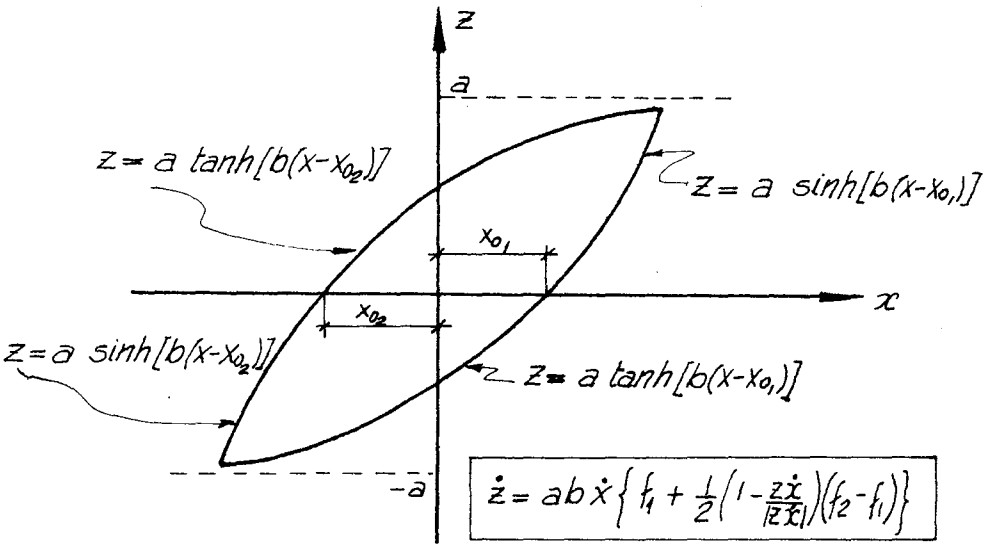

Fig. 15 HYPERBOLIC HYSTERETIC MODEL

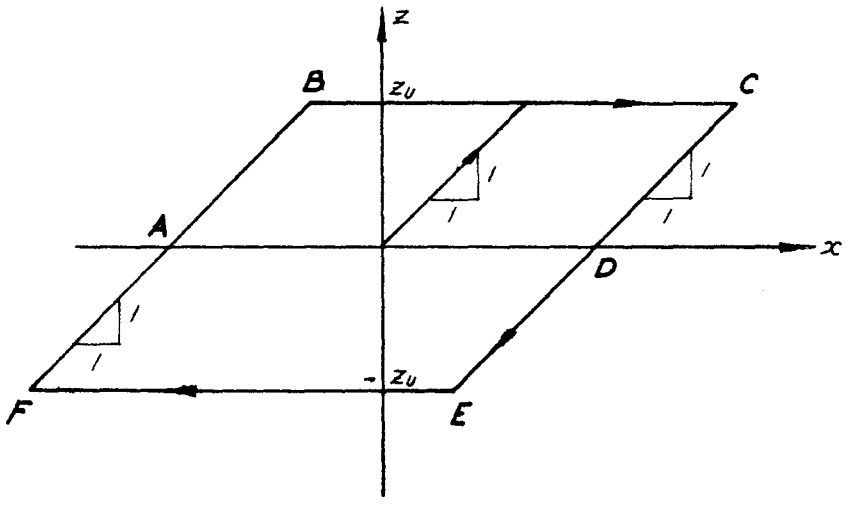

Fig. 16 BILINEAR HYSTERETIC MODEL

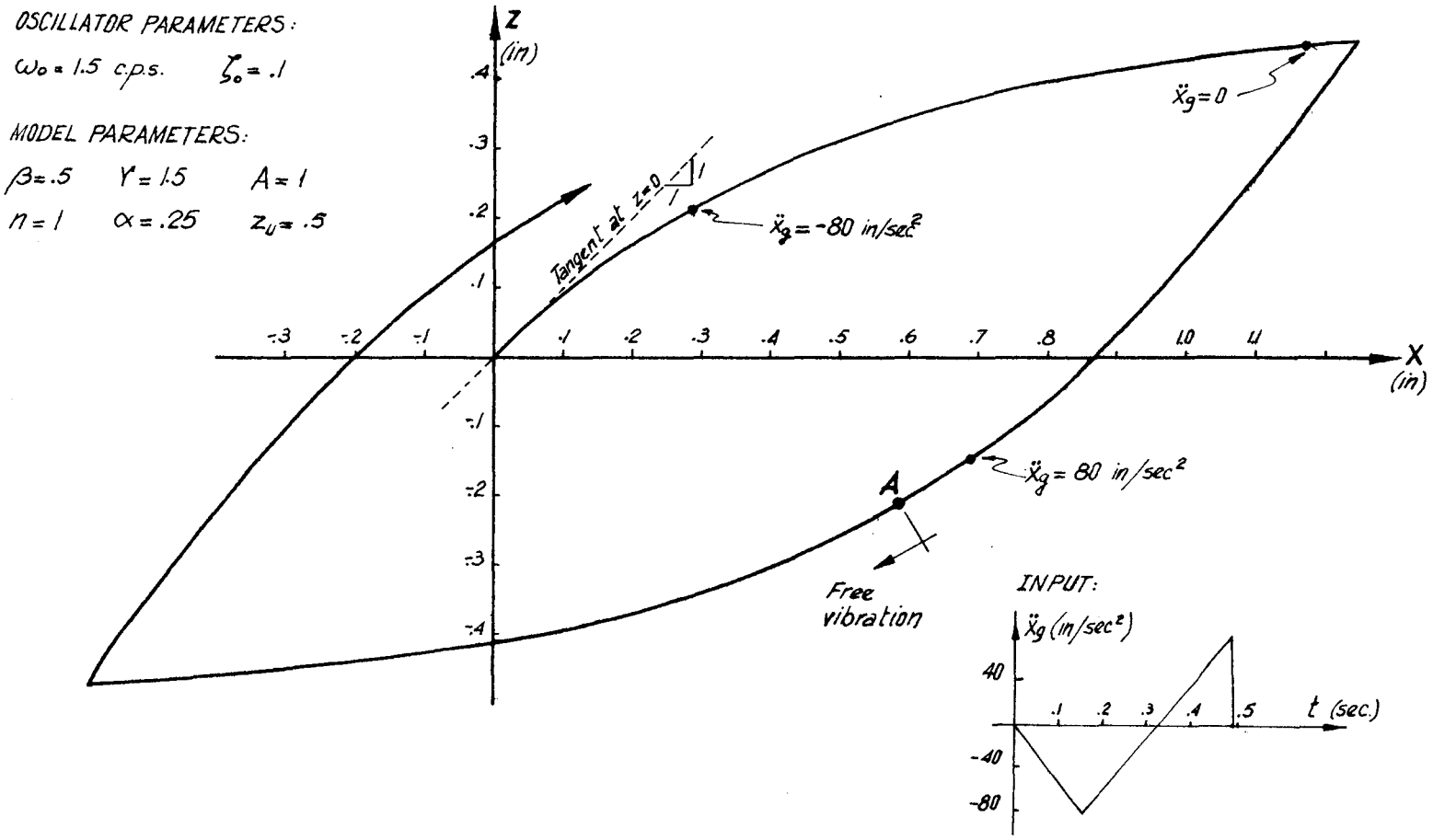

Fig. 17 OSCILLATOR RESPONSE IN THE X-Z PLANE FOR BOUC-WEN MODEL

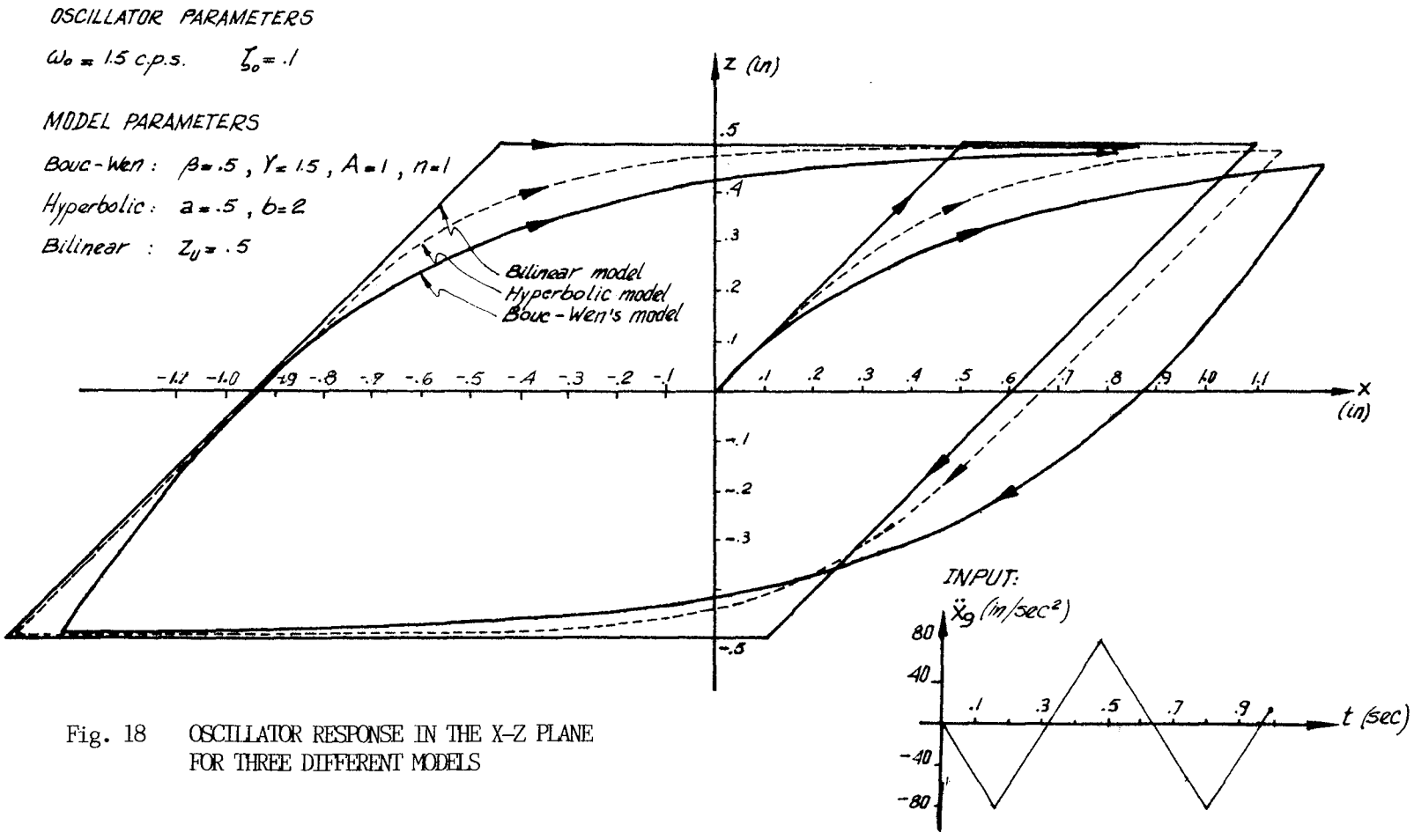

Fig. 18 OSCILLATOR RESPONSE IN THE X–Z PLANE FOR THREE DIFFERENT MODELS

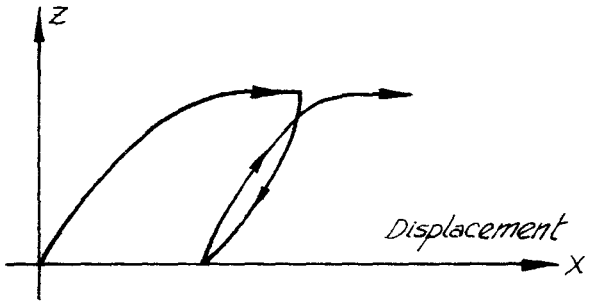

Fig. 19

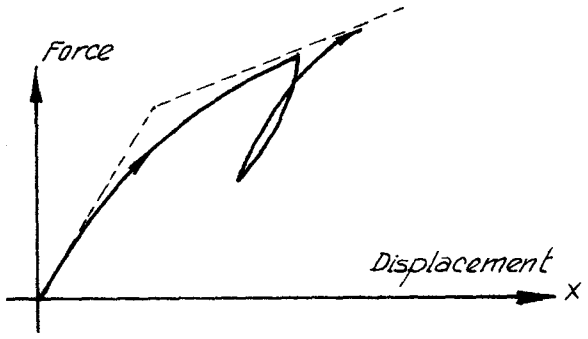

Fig. 20

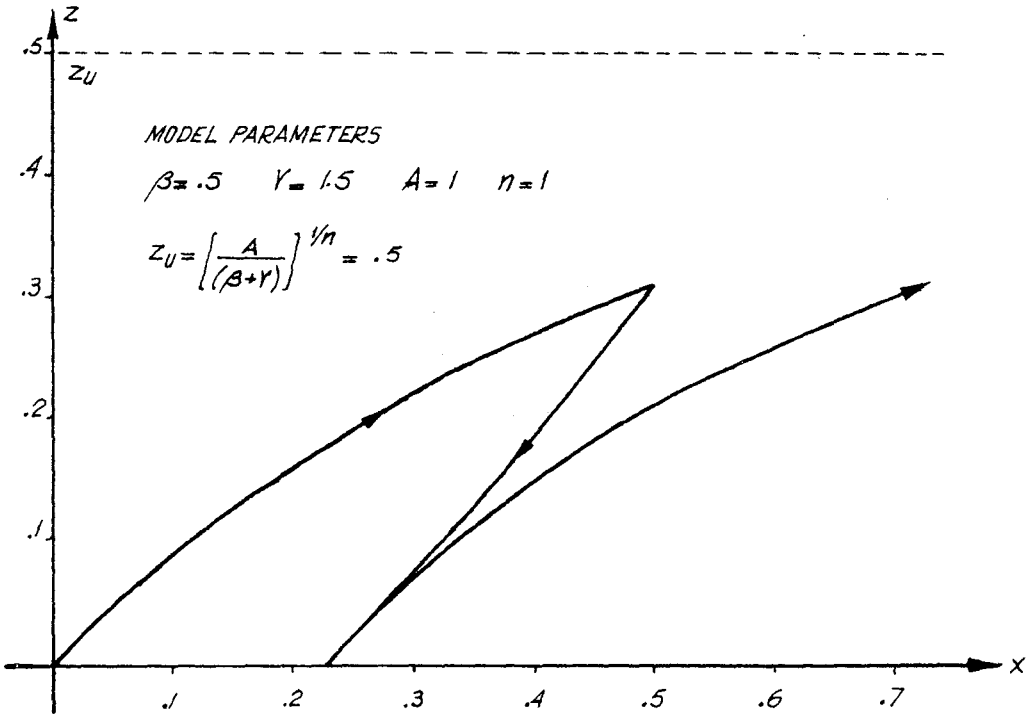

Fig. 21

Oscillator Parameters:

$\omega_0 = 1.0$ rad/sec
$\zeta_0 = .05$
$y = .80$ in
$\alpha = 1/21$

Model Parameters :

$\beta = \gamma$
$A = 1$

INPUT: { —□—□—□— : UNIMODAL
—×—×—×— : TRIMODAL

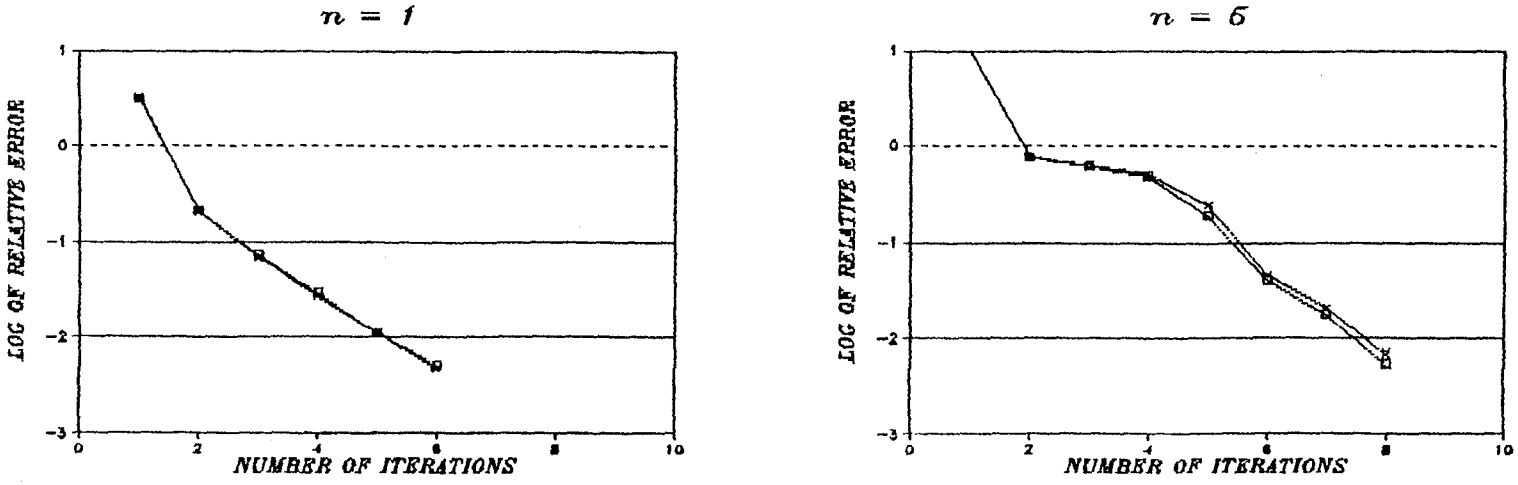

Fig. 22 RATE OF CONVERGENCE

Oscillator Parameters:

$\omega_0 = 1.0$ rad/sec
$\zeta_0 = .05$
$y = .40$ in
$\alpha = 1/21$

Model Parameters :

$\beta = \gamma$
$A = 1$

INPUT: { —□—□—□— : UNIMODAL
—×—×—×— : TRIMODAL

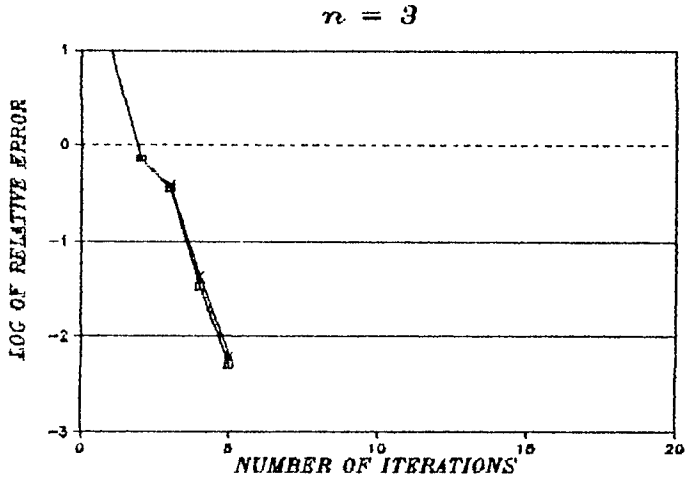

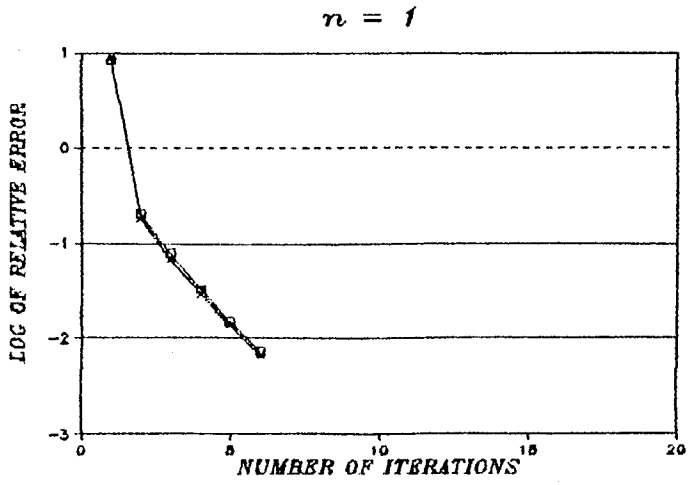

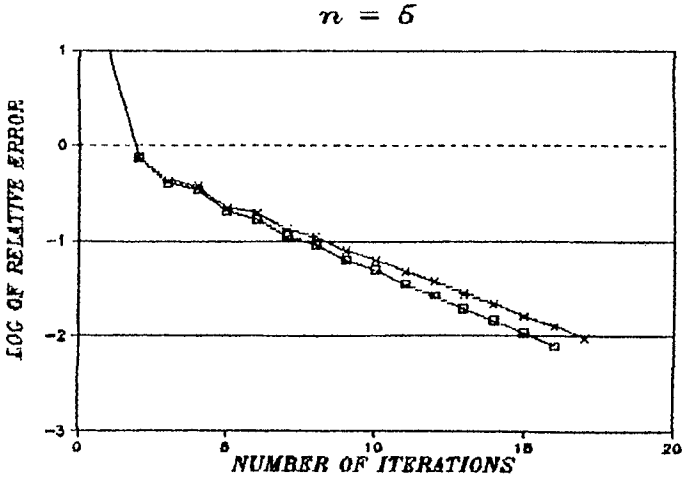

Fig. 23 RATE OF CONVERGENCE

Oscillator Parameters:

$\omega_0 = 1.0$ rad/sec
$\zeta_0 = .05$
$y = .30$ in
$\alpha = 1/21$

Model Parameters :

$\beta = \gamma$
$A = 1$

INPUT: { —□—□—□— : UNIMODAL
—×—×—×— : TRIMODAL

* Initial values of order one.

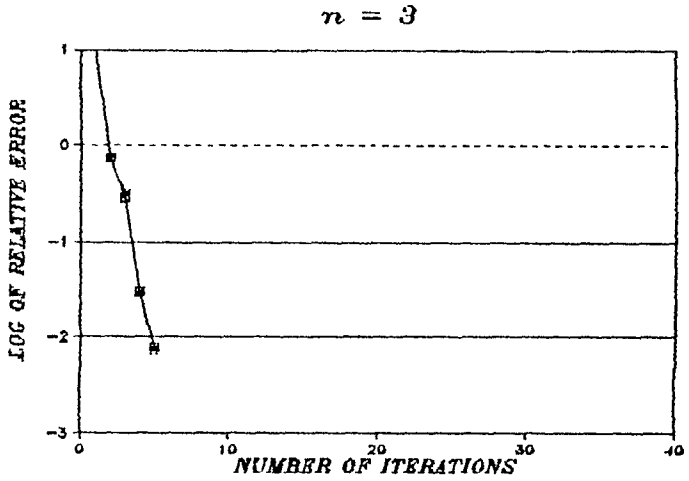

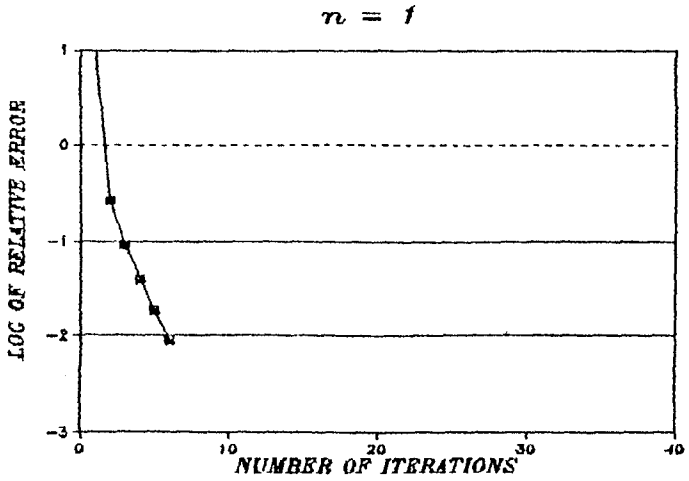

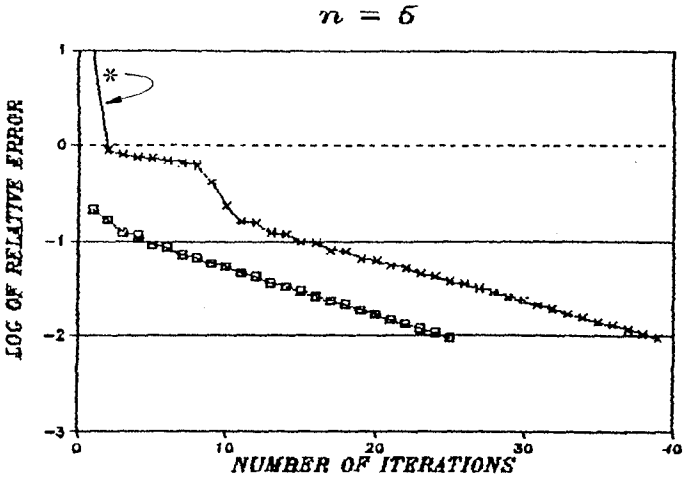

Fig. 24 RATE OF CONVERGENCE

Oscillator Parameters:

$\omega_0 = 5.0$ rad/sec
$\zeta_0 = .05$
$y = .12$ in
$\alpha = 1/21$

Model Parameters :

$\beta = \gamma$
$A = 1$

INPUT: { —□—□—□— : UNIMODAL
{ —×—×—×— : TRIMODAL

* Initial values of order one.

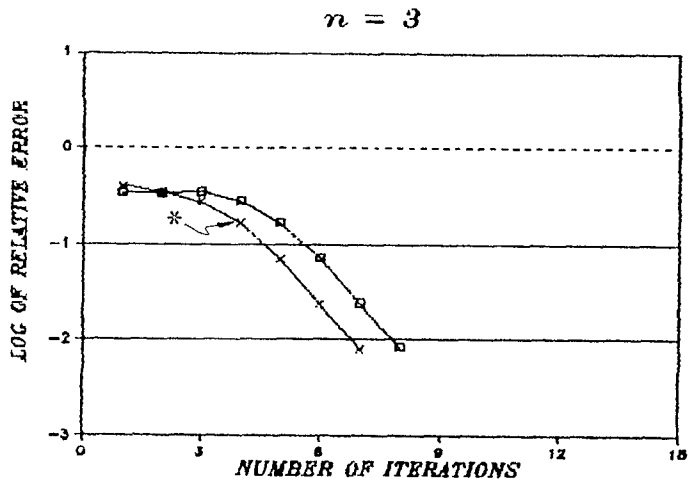

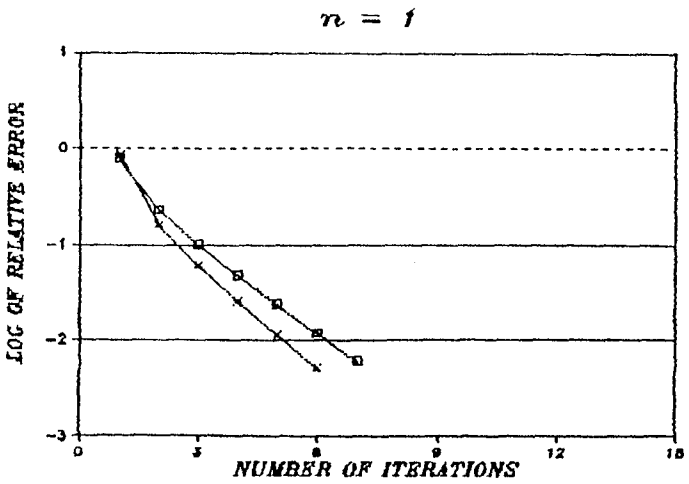

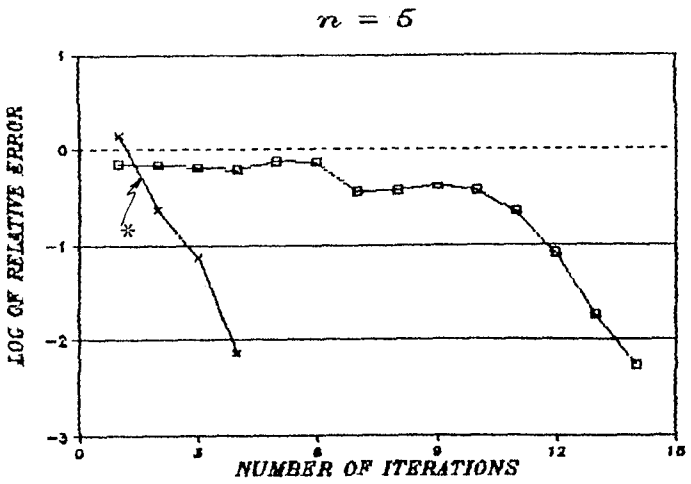

Fig. 25 RATE OF CONVERGENCE

Oscillator Parameters:

$\omega_0 = 5.0$ rad/sec
$\zeta_0 = .05$
$y = .07$ in
$\alpha = 1/21$

Model Parameters :

$\beta = \gamma$
$A = 1$

INPUT: { —□—□—□— : UNIMODAL
—×—×—×— : TRIMODAL

* Initial values of order one.

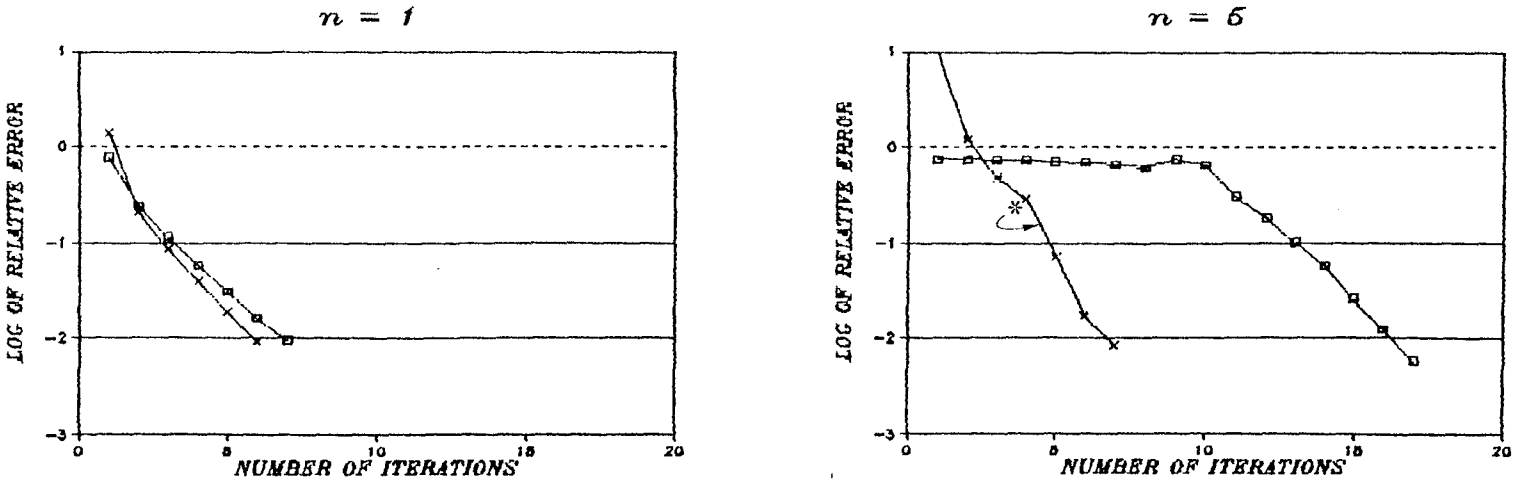

Fig. 26 RATE OF CONVERGENCE

Oscillator Parameters:

$\omega_0 = 5.0$ rad/sec
$\zeta_0 = .05$
$y = .05$ in
$\alpha = 1/21$

Model Parameters :

$\beta = \gamma$
$A = 1$

INPUT: { —□—□—□— : UNIMODAL
{ —×—×—×— : TRIMODAL

* Initial values of order one.

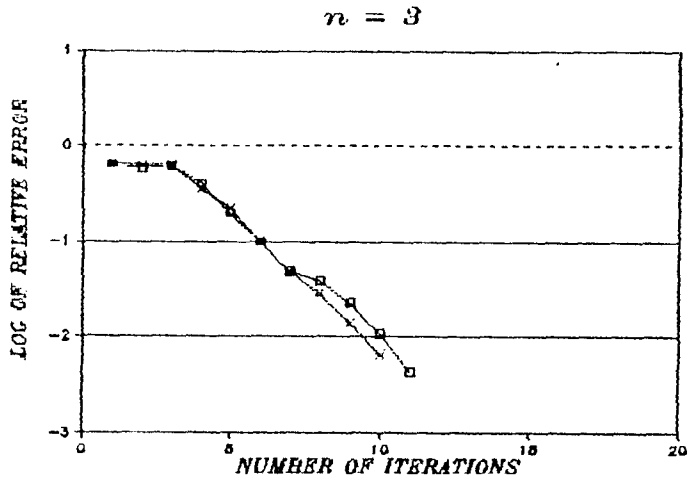

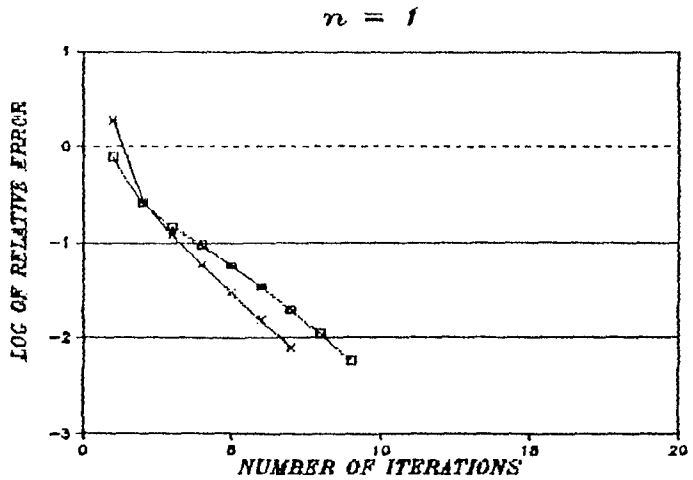

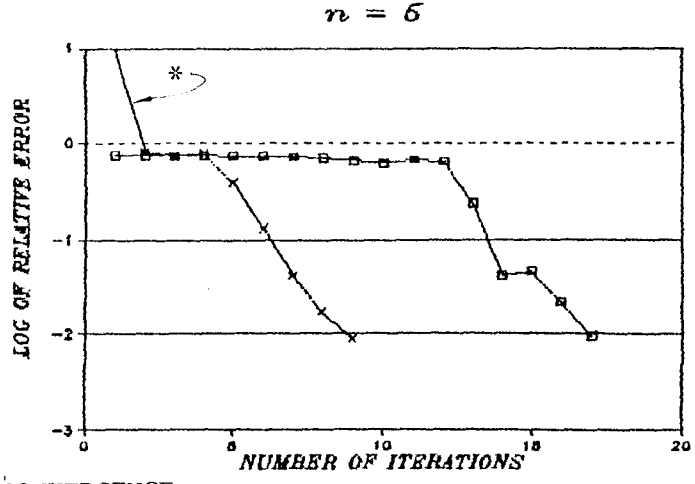

Fig. 27 RATE OF CONVERGENCE

Oscillator Parameters:

$\omega_0 = 16.0$ rad/sec
$\zeta_0 = .05$
$y = .008$ in
$\alpha = 1/21$

Model Parameters :

$\beta = \gamma$
$A = 1$

INPUT: { —□—□—□— : UNIMODAL
—×—×—×— : TRIMODAL

* Initial values of order one.

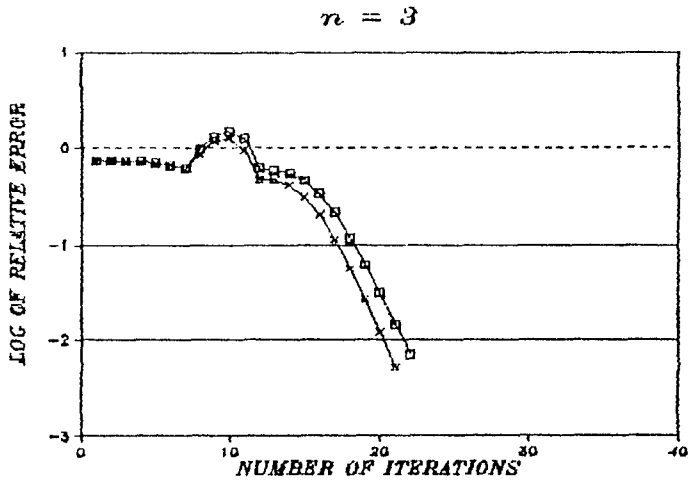

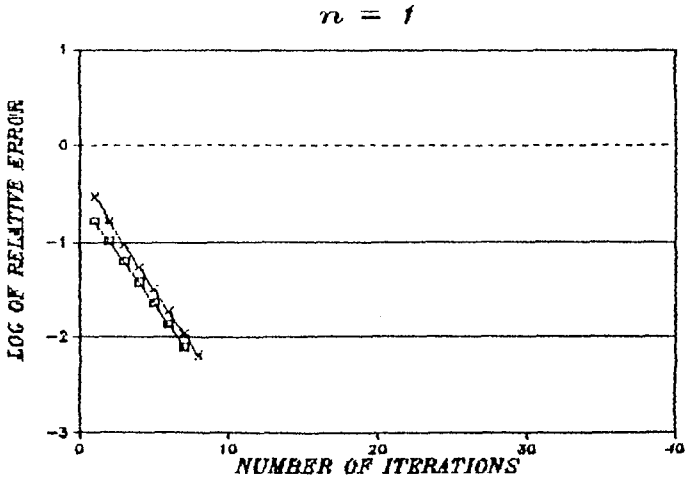

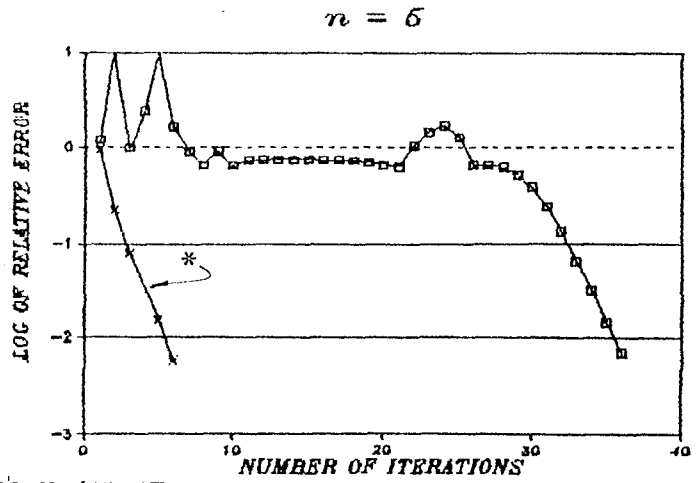

Fig. 28 RATE OF CONVERGENCE

Oscillator Parameters:

$\omega_0 = 16.0$ rad/sec
$\zeta_0 = .05$
$y = .007$ in
$\alpha = 1/21$

Model Parameters :

$\beta = \gamma$
$A = 1$

INPUT: { —□—□—□— : UNIMODAL
{ —×—×—×— : TRIMODAL

* Initial values of order one.

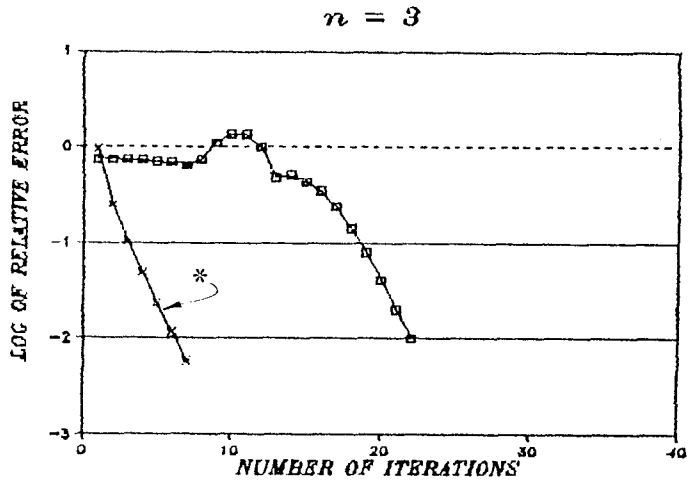

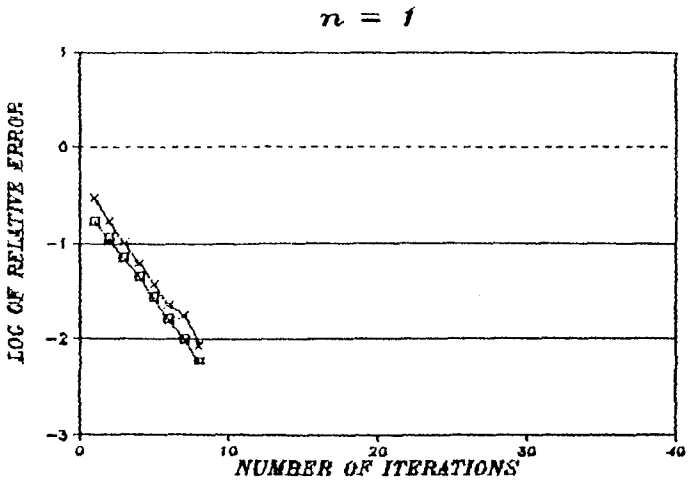

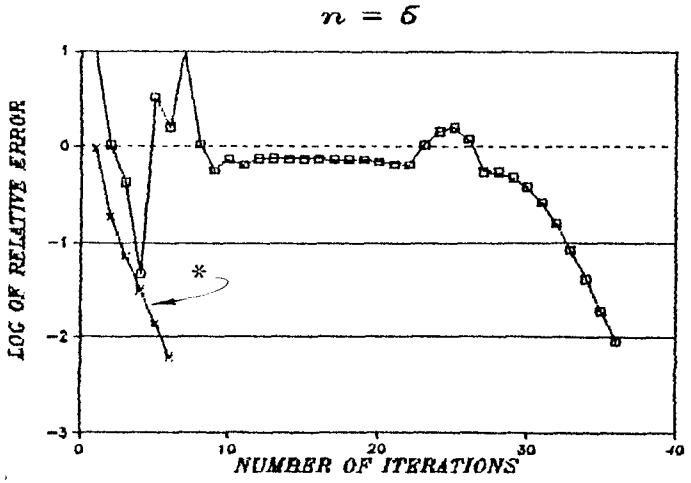

Fig. 29 RATE OF CONVERGENCE

Oscillator Parameters:

$\omega_0 = 1.5$ rad/sec
$\zeta_0 = .10$
$y = .30$ in
$\alpha = .25$

Model Parameters :

$\beta = \gamma$
$A = 1$

INPUT: { —□—□—□— : UNIMODAL
—×—×—×— : TRIMODAL

* Initial values of order one.

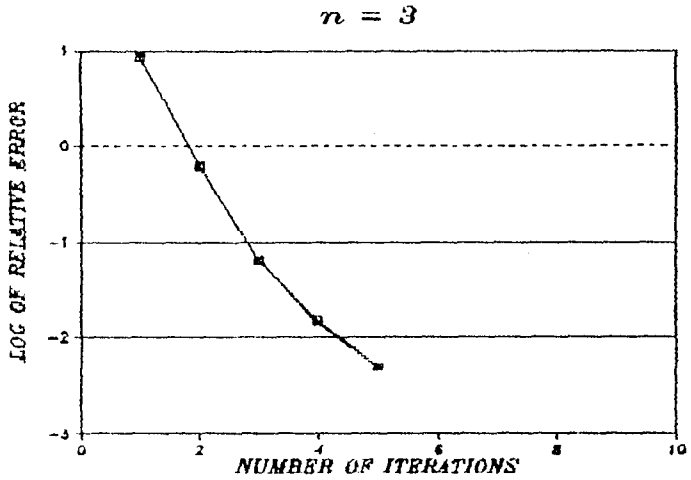

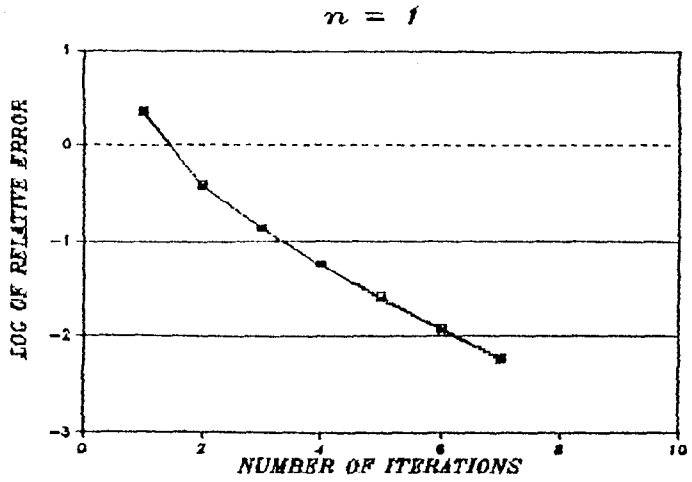

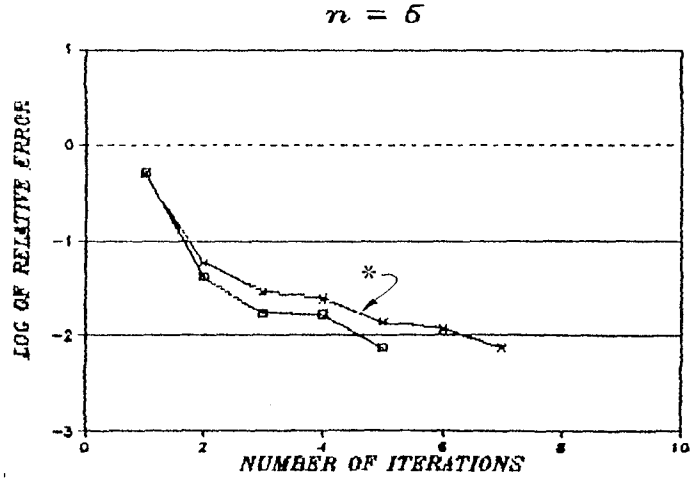

Fig. 30 RATE OF CONVERGENCE

Oscillator Parameters:

ω_0 = 1.5 rad/sec
ζ_0 = .10
y = .20 in
α = .25

Model Parameters :

$\beta = \gamma$
A = 1

INPUT: { —□—□—□— : UNIMODAL
—×—×—×— : TRIMODAL

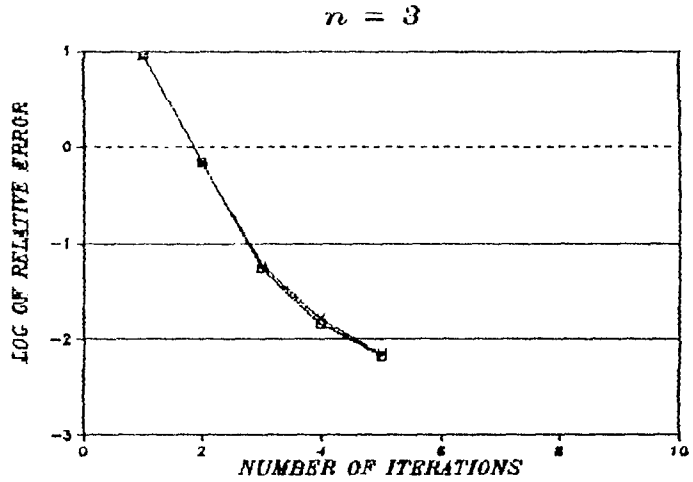

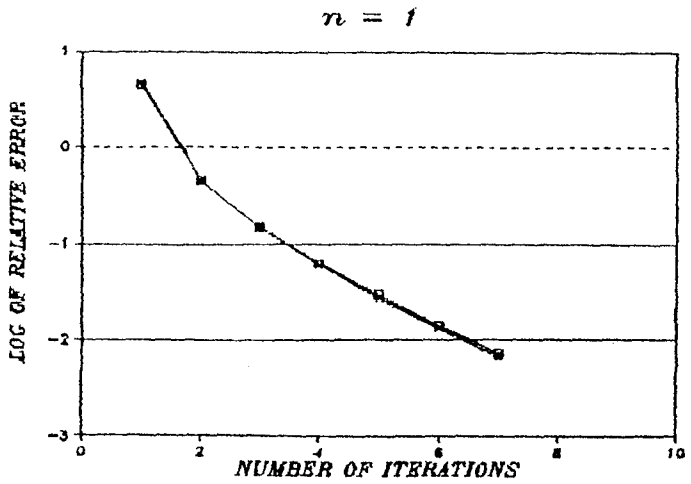

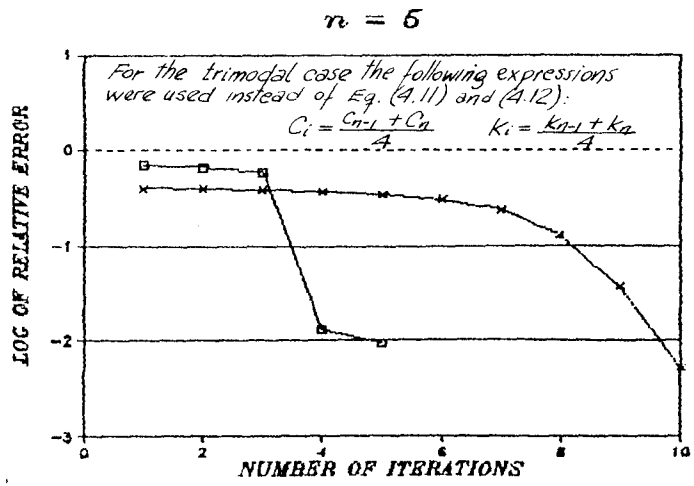

Fig. 31 RATE OF CONVERGENCE

Oscillator Parameters:

$\omega_0 = 6.0$ rad/sec
$\zeta_0 = .10$
$y = .055$ in
$\alpha = .25$

Model Parameters :

$\beta = \gamma$
$A = 1$

INPUT: { —□—□—□— : UNIMODAL
—×—×—×— : TRIMODAL

* Initial values of order one.

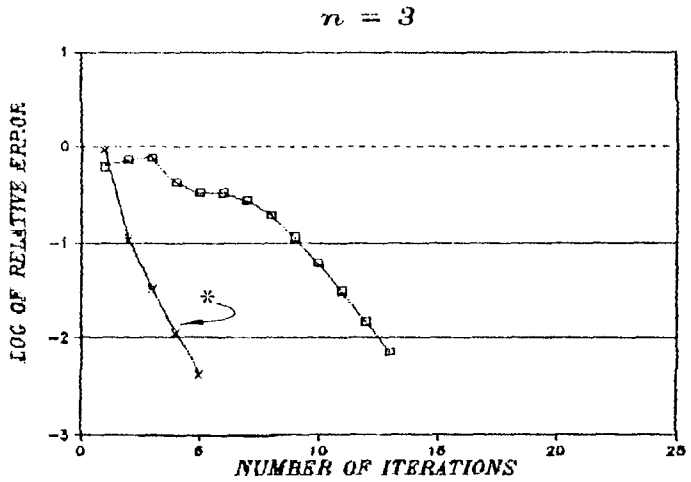

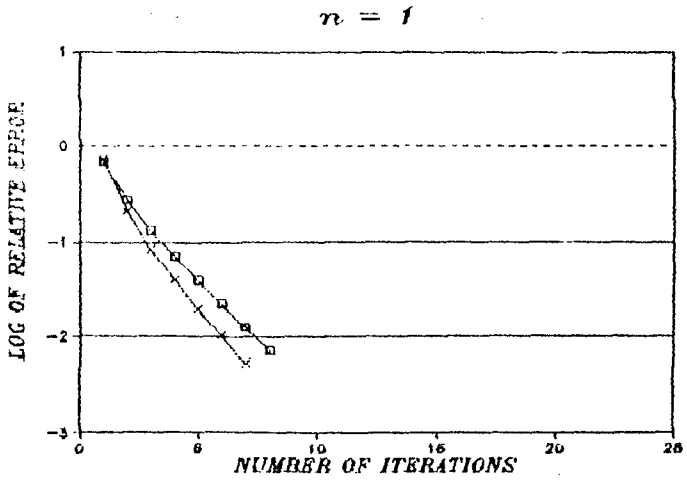

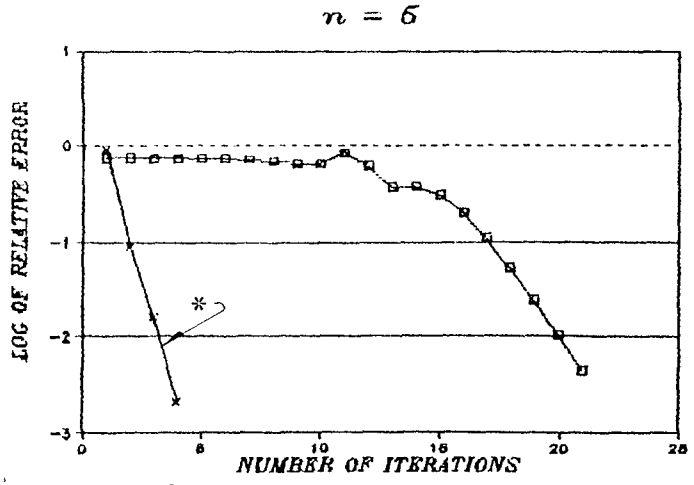

Fig. 32 RATE OF CONVERGENCE

Oscillator Parameters:

ω_0 = 6.0 rad/sec
ζ_0 = .10
y = .032 in
α = .25

Model Parameters :

$\beta = \gamma$
A = 1

INPUT: { —□—□—□— : UNIMODAL
× × × : TRIMODAL

* Initial values of order one.

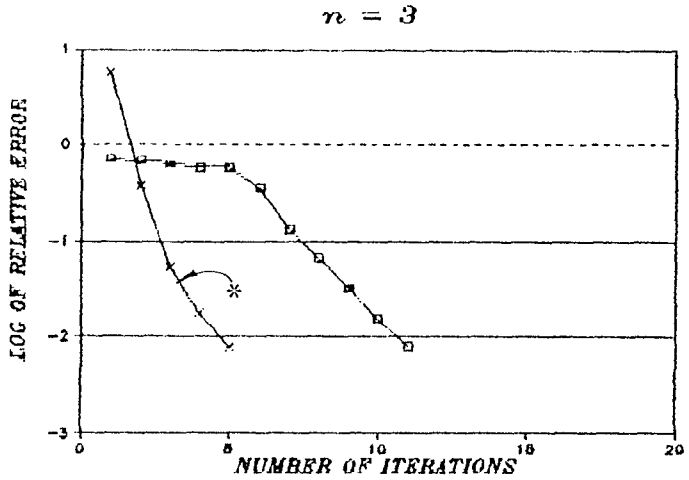

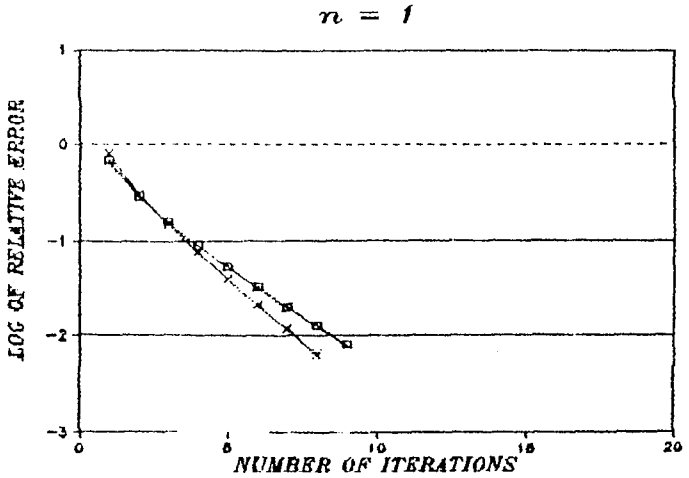

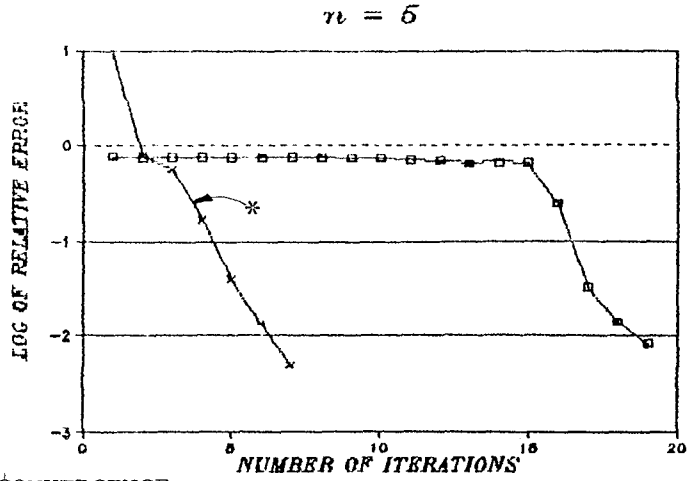

Fig. 33 RATE OF CONVERGENCE

Oscillator Parameters:

ω_0 = 20.0 rad/sec
ζ_0 = .10
y = .0044 in
α = .25

Model Parameters :

$\beta = \gamma$
A = 1

INPUT: { —□—□—□— : UNIMODAL
{ —×—×—×— : TRIMODAL

* Initial values of order one.

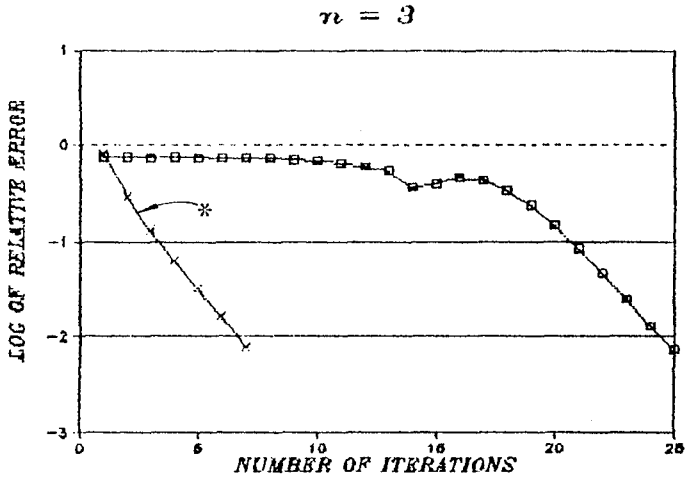

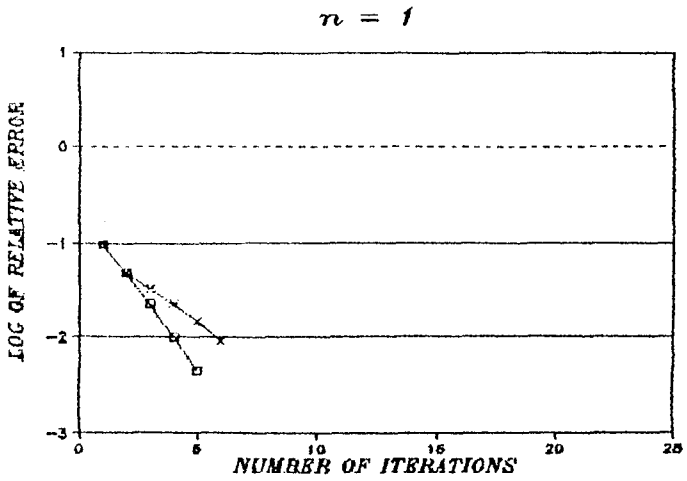

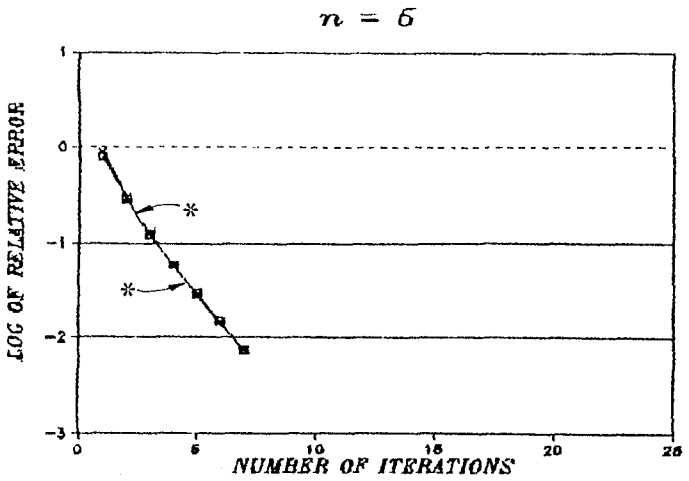

Fig. 34 RATE OF CONVERGENCE

Oscillator Parameters:

$\omega_0 = 20$ rad/sec
$\zeta_0 = .10$
$y = .0036$ in
$\alpha = .25$

Model Parameters :

$\beta = \gamma$
$A = 1$

INPUT: { —□—□—□— : UNIMODAL
{ —×—×—×— : TRIMODAL

* Initial values of order one.

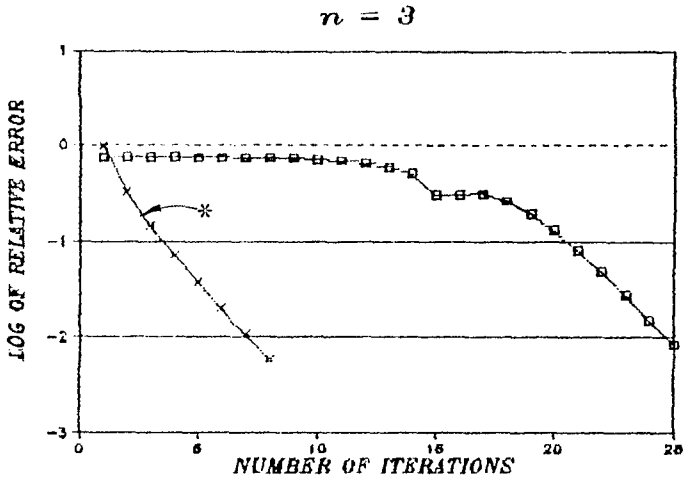

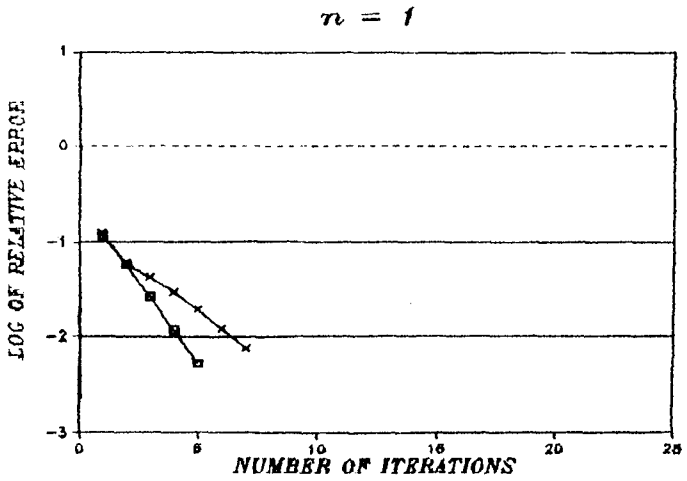

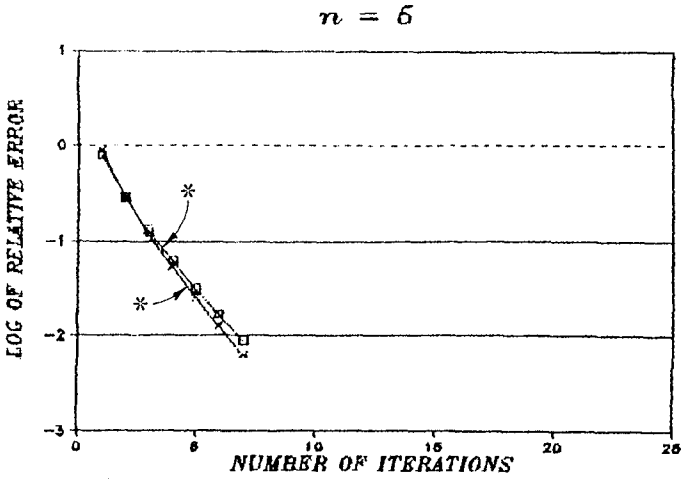

Fig. 35 RATE OF CONVERGENCE

Oscillator Parameters:

$\omega_0 = 20$ rad/sec
$\zeta_0 = .10$
$y = .003$ in
$\alpha = .25$

Model Parameters :

$\beta = \gamma$
$A = 1$

INPUT: { —□—□—□— : UNIMODAL
{ —×—×—×— : TRIMODAL

* Initial values of order one.

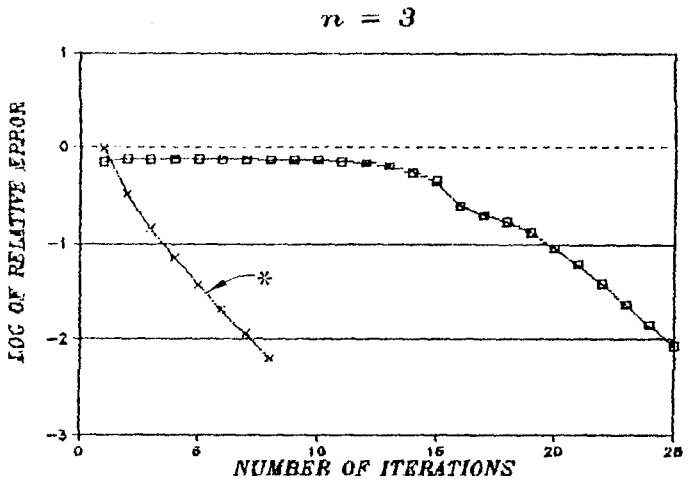

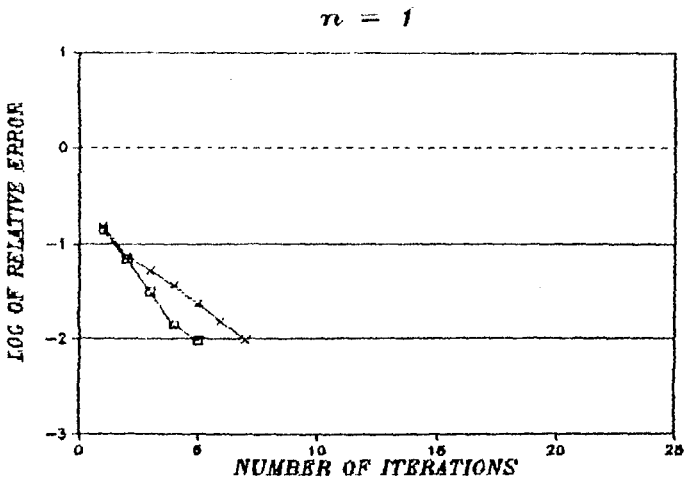

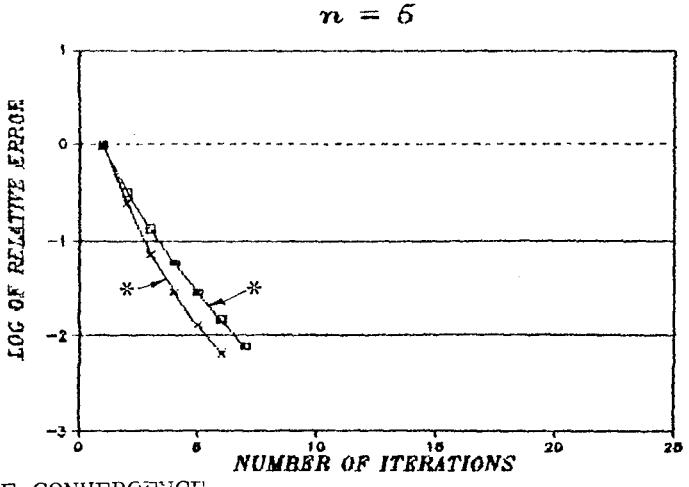

Fig. 36 RATE OF CONVERGENCE

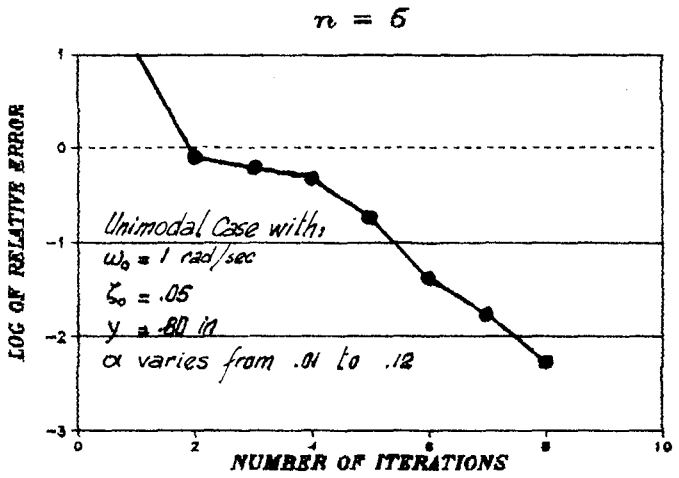
n = 6
LOG OF RELATIVE ERROR
NUMBER OF ITERATIONS
Unimodal Case with,
ω_0 = 1 rad/sec
ζ_0 = .05
y = .80 in
α varies from .01 to .12

Fig. 37

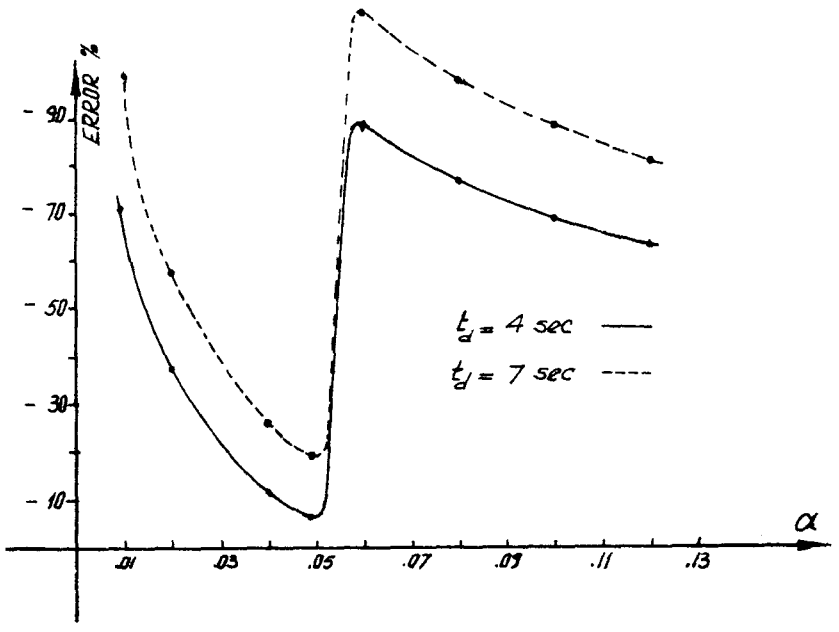
ERROR %
α
t_d = 4 sec
t_d = 7 sec

Fig.38

TABLES

TABLE 01 PARAMETERS FOR THE SPECTRAL DENSITY FUNCTIONS

Unimodal Kanai-Tajimi:

ω_3 =	17.64	rad/sec
ζ_3 =	.3535	
S_3 =	.34125	$(in/sec^2)^2/(rad/sec)$

Trimodal Kanai-Tajimi:

ω_1 =	13.50	rad/sec
ζ_1 =	.3925	
S_1 =	.21600	$(in/sec^2)^2/(rad/sec)$
ω_2 =	23.50	rad/sec
ζ_2 =	.3600	
S_2 =	.07128	$(in/sec^2)^2/(rad/sec)$
ω_3 =	39.00	rad/sec
ζ_3 =	.3350	
S_3 =	.05400	$(in/sec^2)^2/(rad/sec)$

TABLE 02: COMPARISON OF RESULTS — 1 – Modal Case — $\alpha = 1/21$ — $t_d = 4$ sec

Fig.	ω_o (c.p.s.)	ζ_o	y (in)	n = 1			n = 3			n = 5		
				Peak Factor	x_{max} (in)	Error %	Peak Factor	x_{max} (in)	Error %	Peak Factor	x_{max} (in)	Error %
22	1	.05	.800	2.052	1.863	- 9.41	1.336	1.784	- 4.81	2.039	1.812	- 6.44
23	1	.05	.400	1.836	2.294	-15.70	1.772	2.402	-21.18	1.732	2.552	-28.73
24	1	.05	.300	1.503	2.614	-17.41	1.698	2.811	-26.24	1.676	2.981	-33.88
25	5	.05	.120	2.721	0.179	21.14	2.803	0.156	31.03	2.818	0.154	32.15
26	5	.05	.070	2.623	0.213	26.20	2.630	0.190	34.20	2.580	0.197	31.77
27	5	.05	.050	2.538	0.259	28.58	2.478	0.255	29.62	2.437	0.276	24.05
28	16	.05	.008	2.800	0.019	0.60	2.956	0.133	29.20	3.001	0.012	35.62
29	16	.05	.007	2.768	0.020	25.26	2.898	0.015	44.51	2.923	0.014	47.53
Average Error						18.04			27.60			30.02

TABLE 03: COMPARISON OF RESULTS 1 - Modal Case α = .25 t_d = 4 sec

Fig.	ω_0 (c.p.s.)	ζ_0	y (in)	n = 1			n = 3			n = 5		
				Peak Factor	x_{max} (in)	Error %	Peak Factor	x_{max} (in)	Error %	Peak Factor	x_{max} (in)	Error %
30	1.5	.10	.3000	1.850	0.653	29.24	2.362	0.818	11.37	2.334	0.830	10.05
31	1.5	.10	.2000	2.320	0.900	4.16	2.292	0.918	2.34	2.273	0.948	- 0.90
32	6	.10	.0550	2.793	0.089	18.30	2.829	0.080	26.89	2.830	0.079	27.87
33	6	.10	.0320	2.730	0.110	13.22	2.695	0.110	12.72	2.674	0.122	3.00
34	20	.10	.0044	2.947	0.008	8.47	3.023	0.006	25.93	3.040	0.006	29.05
35	20	.10	.0036	2.920	0.008	23.55	2.974	0.007	35.83	2.970	0.007	35.80
36	20	.10	.0030	2.891	0.009	31.42	2.905	0.008	37.38	2.859	0.009	30.74
Average Error						18.34			21.78			19.63

TABLE 04: COMPARISON OF RESULTS — 3 - Modal Case — α = 1/21 — t_d = 4 sec

Fig.	ω_o (c.p.s)	ζ_o	y (in)	n = 1			n = 3			n = 5		
				Peak Factor	x_{max} (in)	Error %	Peak Factor	x_{max} (in)	Error %	Peak Factor	x_{max} (in)	Error %
22	1	.05	.800	2.049	1.880	- 7.38	2.074	1.804	- 3.08	2.030	1.833	- 4.69
23	1	.05	.400	1.832	2.306	-16.32	1.766	2.412	-21.63	1.728	2.552	-28.70
24	1	.05	.300	1.747	2.624	-17.84	1.694	2.813	-26.36	1.673	2.980	-33.84
25	5	.05	.120	2.752	0.191	-15.59	2.825	0.179	-21.14	2.830	0.178	21.59
26	5	.05	.070	2.648	0.215	25.53	2.660	0.200	30.87	2.615	0.205	29.02
27	5	.05	.050	2.559	0.248	31.14	2.508	0.247	31.90	2.456	0.265	26.88
28	16	.05	.008	2.845	0.023	-20.74	2.981	0.017	9.33	2.990	0.016	14.28
29	16	.05	.007	2.813	0.025	8.63	2.903	0.019	28.45	2.891	0.019	27.91
Average Error						17.96			21.60			23.36

TABLE 05: COMPARISON OF RESULTS — 3 – Modal Case — $\alpha = .25$ — $t_d = 4$ sec

Fig.	ω_0 (c.p.s.)	ζ_0	y (in)	n = 1			n = 3			n = 5		
				Peak Factor	x_{max} (in)	Error %	Peak Factor	x_{max} (in)	Error %	Peak Factor	x_{max} (in)	Error %
30	1.5	.10	.3000	2.365	0.847	- 8.25	2.350	0.822	10.90	2.323	0.833	9.78
31	1.5	.10	.2000	2.310	0.908	3.35	2.282	0.922	1.90	2.263	0.951	- 1.22
32	6	.10	.0550	2.846	0.104	5.47	2.873	0.097	11.16	2.863	0.096	12.27
33	6	.10	.0320	2.775	0.117	7.05	2.744	0.116	7.71	2.714	0.123	2.20
34	20	.10	.0044	3.001	0.009	- 6.62	3.068	0.007	12.75	3.076	0.007	14.79
35	20	.10	.0036	2.972	0.010	10.18	3.009	0.008	22.44	2.983	0.009	18.78
36	20	.10	.0030	2.944	0.010	18.99	2.937	0.010	22.99	2.887	0.011	13.19
Average Error						8.56			12.84			10.32

TABLE 06: COMPARISON OF RESULTS — 1 – Modal Case — α = 1/21 — t_d = 7 sec

Fig.	ω_o (c.p.s.)	ζ_o	y (in)	n = 1			n = 3			n = 5		
				Peak Factor	x_{max} (in)	Error %	Peak Factor	x_{max} (in)	Error %	Peak Factor	x_{max} (in)	Error %
22	1	.05	.800	2.301	2.090	-22.75	2.328	1.996	-17.26	2.290	2.035	-19.54
23	1	.05	.400	2.106	2.631	-32.68	2.046	2.775	-39.95	2.009	2.961	-49.33
24	1	.05	.300	1.740	3.026	-35.91	1.977	3.272	-46.98	1.956	3.478	-56.22
25	5	.05	.120	2.918	0.192	15.44	2.995	0.167	26.31	3.009	0.164	27.55
26	5	.05	.070	2.827	0.230	20.47	2.833	0.205	29.12	2.787	0.213	26.30
27	5	.05	.050	2.747	0.281	22.68	2.692	0.277	23.54	2.654	0.300	17.28
28	16	.05	.008	2.992	0.020	- 6.22	3.138	0.014	24.83	3.181	0.013	31.76
29	16	.05	.007	2.962	0.021	20.02	3.084	0.016	40.95	3.108	0.015	42.22
Average Error						22.02			31.12			34.03

TABLE 07: COMPARISON OF RESULTS — 1 - Modal Case — $\alpha = .25$ — $t_d = 7$ sec

Fig.	ω_0 (c.p.s.)	ζ_0	y (in)	n = 1			n = 3			n = 5		
				Peak Factor	x_{max} (in)	Error %	Peak Factor	x_{max} (in)	Error %	Peak Factor	x_{max} (in)	Error %
30	1.5	.10	.3000	2.118	0.748	18.98	2.585	0.895	2.99	2.560	0.910	1.36
31	1.5	.10	.2000	2.547	0.988	- 5.20	2.520	1.009	- 7.41	2.503	1.044	-11.13
32	6	.10	.0550	2.985	0.096	12.67	3.019	0.085	21.98	3.020	0.084	23.02
33	6	.10	.0320	2.927	0.117	6.98	2.894	0.118	6.28	2.655	0.132	- 4.26
34	20	.10	.0044	3.130	0.008	2.78	3.202	0.006	21.55	3.218	0.006	24.89
35	20	.10	.0036	3.104	0.009	18.71	3.156	0.007	31.90	3.152	0.007	31.87
36	20	.10	.0030	3.078	0.009	27.00	3.091	0.009	33.38	3.047	0.010	26.18
Average Error						13.19			17.93			17.53

TABLE 08: COMPARISON OF RESULTS — 3-Modal Case — α = 1/21 — t_d = 7 sec

Fig.	ω_o (c.p.s.)	ζ_o	y (in)	n = 1			n = 3			n = 5		
				Peak Factor	x_{max} (in)	Error %	Peak Factor	x_{max} (in)	Error %	Peak Factor	x_{max} (in)	Error %
22	1	.05	.800	2.299	2.109	-20.49	2.322	2.020	-15.40	2.282	2.060	-17.69
23	1	.05	.400	2.102	2.645	-33.43	2.041	2.787	-40.58	2.005	2.961	-49.36
24	1	.05	.300	2.023	3.038	-36.47	1.973	3.277	-47.18	1.953	3.478	-56.21
25	5	.05	.120	2.947	0.205	- 9.61	3.015	0.191	15.32	3.020	0.190	16.33
26	5	.05	.070	2.850	0.232	19.85	2.861	0.215	25.64	2.819	0.221	23.48
27	5	.05	.050	2.767	0.268	26.08	2.719	0.268	26.15	2.672	0.289	20.46
28	16	.05	.008	3.034	0.024	-28.77	3.162	0.018	3.82	3.171	0.017	9.10
29	16	.05	.007	3.079	0.026	2.43	3.089	0.020	23.88	3.078	0.021	23.26
Average Error						22.14			24.81			26.99

TABLE 09: COMPARISON OF RESULTS — 3 – Modal Case — α = .25 — t_d = 7 sec

Fig.	ω_0 (c.p.s.)	ζ_0	y (in)	n = 1			n = 3			n = 5		
				Peak Factor	x_{max} (in)	Error %	Peak Factor	x_{max} (in)	Error %	Peak Factor	x_{max} (in)	Error %
30	1.5	.10	.3000	2.588	0.927	- 0.39	2.514	0.901	2.41	2.550	0.914	1.00
31	1.5	.10	.2000	2.538	0.997	- 6.16	2.511	1.014	- 7.98	2.494	1.048	-11.57
32	6	.10	.0550	3.035	0.110	- 0.82	3.061	0.104	5.36	3.051	0.102	6.50
33	6	.10	.0320	2.968	0.126	0.56	2.940	0.125	1.14	2.911	0.132	- 4.91
34	20	.10	.0044	3.181	0.009	-13.02	3.245	0.008	- 7.73	3.252	0.007	9.91
35	20	.10	.0036	3.154	0.010	4.69	3.189	0.009	17.88	3.164	0.009	13.85
36	20	.10	.0030	3.127	0.011	13.94	3.120	0.011	18.18	3.073	0.012	7.57
Average Error						5.65			8.67			7.90

REFERENCES

1. A. E. Kanaan and G. H. Powell, "DRAIN-2D General Purpose Program for Dynamic Analysis of Inelastic Plane Structures", Earthquake Engineering Research Center, Report No. EERC 73-6 and EERC 72-22, University of California, Berkeley, April 1973.

2. D. P. Monkar and G. H. Powell, "ANSR-1 General Purpose Program for Analysis of Nonlinear Structural Response", Earthquake Engineering Research Center, Report No. EERC 75-37, University of California, Berkeley, December 1975.

3. W. Ramberg and W. T. Osgood, "Description of Stress-strain curves by Three Parameters", Technical Note 902, National Advisory Committee for Aeronautics, 1943.

4. E. Faccioli and J. Ramirez, "Earthquake response of Non-linear hysteretic Soil Systems, Earthquake Engineering and Structural Dynamics, Vol 4, 261-276, 1976.

5. M. P. Singh and Ghafory-Ashtiany, "Seismically Induced Stresses and Stability of Soil Media", Soil Dynamics and Earthquake Engineering, Vol. 1, No. 4, 167-177, 1982.

6. W. D. Iwan, "The Distributed Element Concept of Hysteretic Modeling and its Application to Transient Response Problems", Procedings of the Fourth World Conference on Earthquake Engineering, Vol. II, A-4, 45-47, Santiago, Chile, 1969.

7. R. Bouc, "Forced Vibration of Mechanical Systems with Hysteresis", Abstract, Procedings of the Fourth Conference on Nonlinear Oscillation, Prague, Czechoslovakia, 1967.

8. H. Ozdemir, "Nonlinear Transient Dynamic Analysis of Yielding Structures", Ph. D. Dissertation, Division of Structural Engineering and Structural Mechanics, Department of Civil Engineering, University of California, Berkeley, 1976.

9. M. A. Bhatti and K. S. Pister, "A Dual Criteria Approach for Optimal Design of Earthquake-resistant Structural Systems", Earthquake Engineering and Structural Dynamics, Vol. 9, 557-572, 1981.

10. Y. K. Wen, "Method for Random Vibration of Hysteretic Systems", Engineering Mechanics Division, Proceedings, ASCE, Vol. 102, No. EM2, 249-263, April 1976.

11. T. T. Baber and Y. K. Wen "Stochastic Equivalent Linearization for Hysteretic, Degrading, Multistory Structures", Report Submitted to the National Science Foundation, Research Grant ENV 77-09090, April 1980.

12. F. Casciati and L. Faravelli, "Non-linear Sthocastic Dynamics by Equivalent Linearization", Department of Structural Mechanics, University of Pavia, Italy, 1986.

13. F. Casciati, "Equivalent Linearization Technique in the Analysis of Seismic-excited Structures", Procedings of the Euro-China Joint Seminar on Earthquake Engineering, Beijing, June 1986.

14. T. S. Atalik and S. Utku, "Stochastic Linearization of Multi-degree-of-freedom Non-linear Systems", Earthquake Engineering and Structural Dynamics, Vol. 4, 411-420, 1976.

15. Y. K. Wen, "Equivalent Linearization for Hysteretic Systems Under Random Excitation", Applied Mechanics, Vol 47, 150-154, March 1980.

16. N. Krylov and N. Bogoliubov, "Introduction to Nonlinear Mechanics", Princeton, New Jersey, Translated from 1937 Russian Edition.

17. Y. K. Lin, "Probabilistic Theory of Structural Dynamics", Mc Graw-Hill, New York, 1967.

18. R. H. Bartels and G. W. Steward, "Solution of the Matrix Equation AX + XB = C", Communication of the ACM, Vol. 15, No. 9, 820-826.

19. U.S. Nuclear Regulatory Commission: "Design Response Spectra for Nuclear Power Plants", Nuclear Regulatory Guide, No. 1.60, Washington, D.C., 1975.

20. M. P. Singh and S. L. Chu, "Stochastic Considerations in Seismic Analysis of Structures", Earthquake Engineering Structural Dynamics, Vol. 4, 295-307, 1976.

21. S. R. Malushte, "Seismic Design Response of Simple Nonlinear Hysteretic Structures", M. S. Thesis, Virginia Polytechnic Institute and State University, September 1984.

22. F. Casciati, Personal communication.

23. A. G. Davenport, "Note on the Distribution of the Largest Value of a Random Function with Application to Gust Loading, Proc. Inst. Civil Engineering, Vol. 28, 187-196.